Alma Mater Studiorum – Università di Bologna

DOTTORATO DI RICERCA IN

SCIENZE E TECNOLOGIE AGRARIE, AMBIENTALI E ALIMENTARI

Ciclo XXXII

Settore Concorsuale: 07/B2

Settore Scientifico Disciplinare: AGR/05

USE OF SENTINEL 2 SATELLITE IMAGERY FOR FOREST SITE EVALUATION AND FOREST HARVESTING DETECTION

Presentata da: **Nicola Sangiorgi**

Coordinatore Dottorato
Prof. Massimiliano Petracci

Supervisore
Federico Magnani

Esame finale anno 2020

"Going to the mountains
is going home"

John Muir – The mountains of California, 1894

Preface and acknowledgement

This thesis describes the work done during the three years Ph.D. student position of the author. This period was spent mainly at University of Bologna, which completely founded this research and supported the collaboration with the Center for Global Discovery and Conservation Science (GDCS - https://gdcs.asu.edu/) at Arizona State University.

A key part of this study was the databased with ground-truth information about forest harvesting in the province of Bologna. The creation of this database was achieved with the helpful information gathered from institutions, cooperatives and loggers. We acknowledge for that a large number of people such as Dott. For. Alessandra Pesino (Unione dei Comuni dell'Appennino Bolognese), the staff of Protected Areas, Forests and Mountain Development Service in the Emilia Romagna institution, Dott. Alvaro Pederzoli (Unione dei Comuni della Romagna Faentina), Dott. Geol. Pier Luigi Maschietto and Dott. Fabiano Molinari (ATERSIR). Some foresters freelance: Dott. For. Agostino Barbieri, Dott. For. Antonio Mortali and a long list of loggers: Marius Isai, Romeo Nesti, Paolo Barrottu, Moreno Bartolini, Matteo Bernardini, Claudio Lazzarini.

Additionally, we recognize the great usefulness of meetings and discussions with Dott. Agr. Andrea Spisni (Arpae Emilia-Romagna), Dott. Cinzia Panigada (Milano Bicocca University), PhD Reiche Johannes (Wageningen University), PhD Luigi Ranghetti (CNR-IREA) and the staff of METEORS lab IFAC-CNR.

Table of Contents

PREFACE AND ACKNOWLEDGEMENT ..... **IV**

TABLE OF CONTENTS ..... **V**

LIST OF FIGURES ..... **VII**

LIST OF TABLES ..... **VIII**

LIST OF EQUATIONS ..... **IX**

ABSTRACT **1**

GENERAL INTRODUCTION **2**

1 REMOTE SENSING: IN GENERAL **2**
2 SOURCES OF ERRORS **4**
3 CONCEPT OF RESOLUTION **5**
4 REMOTE SENSING APPLIED TO FOREST MANAGEMENT **6**
5 AIMS OF THE THESIS **7**
5.1 How to read the thesis *8*
6 BIBLIOGRAPHY **9**

CHAPTER I – SITE INDEX AND GROWTH PREDICTION FROM REMOTE SENSING AND ENVIRONMENTAL FACTORS IN DOUGLAS-FIR PLANTATIONS **14**

1 ABSTRACT **14**
2 INTRODUCTION **15**
3 MATERIALS AND METHODS **16**
3.1 Study area *16*
3.2 Stands data *17*
3.3 Soil variables *18*
3.4 Climatic variables *18*
3.5 Remote sensed variables *19*
3.6 Models development *20*
4 RESULTS **22**
4.1 Site Index *22*
4.2 Net current annual increment *24*
5 DISCUSSION **27**
5.1 Statistical approach *28*
5.2 Factors affecting fertility *28*
6 CONCLUSION **29**
7 BIBLIOGRAPHY **30**

CHAPTER II – EVALUATION OF SENTINEL-2 TIME SERIES CHANGE DETECTION FOR FOREST HARVESTING OF VARIABLE INTENSITY IN TEMPERATE FORESTS **35**

1 ABSTRACT **35**
2 INTRODUCTION **36**
2.1 Optical sensors problems *36*
3 MATERIALS AND METHODS **39**
3.1 Study area *39*
3.2 Bayesian multi-input time series approach *40*
3.3 Calibration and validation dataset *40*
3.4 Sentinel-2 data and pre-process workflow *43*
3.5 Calibration method *45*
3.6 Results assessment *45*

3.7 Change detection algorithm application ... 46
4 RESULTS ... 48
5 DISCUSSION ... 51
6 CONCLUSION ... 55
7 BIBLIOGRAPHY ... 56

CHAPTER III - CHANGE DETECTION WITH BAYTSDD AND BAYTS USING THE ENTIRE TIME SERIES: OVERCOME THE SEASONAL PROBLEM IN TEMPERATE FOREST ... 62

1 ABSTRACT ... 62
2 INTRODUCTION ... 63
3 MATERIALS AND METHODS ... 65
3.1 Study area ... 65
3.2 Satellite data ... 65
3.3 Seasonality removal and pdf estimation for Bayts ... 66
3.4 Seasonality removal and pdf estimation for BaytsDD ... 67
3.5 Bayesian change detection methods: Bayts and BaytsDD ... 68
3.6 Validation ... 68
4 RESULTS AND DISCUSSION ... 70
4.1 BaytsDD change detection accuracy ... 72
4.2 Bayts change detection accuracy ... 73
5 CONCLUSION ... 75
6 BIBLIOGRAPHY ... 76

CHAPTER IV – TIME SERIES CHANGE DETECTION WITH DIFFERENT INPUT SOURCES FOR ASSESSING INCREASING SPATIAL RESOLUTION: SENTINEL-2, CLASLITE, RAPIDEYE AND PLANETSCOPE ... 80

1 INTRODUCTION ... 80
2 MATERIAL AND METHODS ... 81
2.1 CLASlite time series ... 81
2.2 Sentinel-2, RapidEye and Planet Scope time series ... 81
3 RESULTS AND DISCUSSION ... 82
3.1 CLASlite and Sentinel-2 comparison ... 82
3.2 Spatial resolution effect on change detection ... 83
4 CONCLUSION ... 85
5 BIBLIOGRAPHY ... 86

GENERAL CONCLUSION ... 87

List of figures

Figure 1 - Electromagnetic spectrum (Mukesh, 2015). Visible, infrared and microwave are currently the most relevant ranges used in earth observation.....3

Figure 2 - Location of the study area and relative plots for field survey.....16

Figure 3 - Goodness of fit for the best Site Index models:.....24

Figure 4 - Goodness of fit for the best CAI models:.....26

Figure 5 - SEN2COR processor generate Level-2A products with a scene classification for many classes including cloud and cloud shadow (ESA, 2019). from left to right: (1) Sentinel-2 Level-1C TOA reflectance input image, (2) the atmospherically corrected Level-2A BOA reflectance image, (3) the output scene classification of the Level-1C product.....37

Figure 6 - Study area location, in the zoomed window are showed the dataset for calibration and validation.....39

Figure 7 - Database of logging events from 2015 to 2018 for calibrate the probability density functions (yellow) and for validate and assessing (Red) the accuracy for the change detection method.....42

Figure 8 - Validation dataset classified by year (on the left) and harvesting techniques (on the right).....43

Figure 9 - Number of Sentinel-2 images per month with a total amount of 39 images.....44

Figure 10 – NDVI and NBR histogram of frequency for non-forest (red) and forest (green) pixels.....48

Figure 11 - NBR and NDVI change detection maps. In the upper image, two black circles indicate the main commission errors areas due to old harvest areas (before 2015).....53

Figure 12 – Output map from NBR and NDVI time series fuse together.....54

Figure 13 - Number of Sentinel-2 images per month. They represented the whole time series, images with cloud cover lower than 20%. Total amount of image was 76.....65

Figure 14 - Deseasonalization for NBR time series in a single pixel with deciduous vegetation. Not deseasonalizated time series in the middle graph (B). The upper graph (A) illustrates both with and without seasonal effect in the NBR time series, the spatial normalization was applied in order to remove the seasonal effect for the Bayts method. The lower graph (C) shows how the harmonic model applied has removed the seasonal effect in the time series, method for BaytsDD.....70

Figure 15 - Single pixel BaytsDD for NBR time series. Detection error occurred due to seasonal removal error. (A) NBR original time series, (B) NBR deseasonalized time series with start monitoring date (black line) and change detection by error (red line).....72

Figure 16 - Output raster from BaytsDD change detection applied to NBR and NDVI time series. Smaller area was used due to the shorter monitoring period.....74

Figure 17 - Output raster from Bayts change detection using NBR and NDVI time series with spatial normalization.....74

Figure 18 - Calibration probability density function for Forest (green distribution) e Non-Forest (red distribution) area from CLASlite fractional cover. Left: Non-photosynthetic vegetation, Center: Photosynthetic vegetation, Right: Bare soil.....81

Figure 19 - Bayts change detection comparison between NDVI Sentinel-2 input source (left) and fractional cover from CLASlite (right).....82

Figure 20 - Bayts change detection mapping with different spatial resolution NDVI time series. input source from Sentinel-2 (10m) on the left, RapidEye (5 m) in center and Planet Scope (3m) on the right.....84

List of tables

Table 1 - Measured and estimated stands characteristics (value between all 15 plots) *17*

Table 2 - Climate variable statistically relevant to delineate Douglas-fir niche according to Rehfeldt et al. (2014) ... *19*

Table 3 - Input variables list *21*

Table 4 - Site Index models summary. *22*

Table 5 - CAI net models summary *25*

Table 6 – Statistical summary for calibration database, the high number of coppice cut show the importance of this technique in the study area. *41*

Table 7 -Statistical summary for validation database. *43*

Table 8 - Change detection results for spatial and temporal accuracy assessment *49*

Table 9 - Change detection results for simplified classes "cut" "no-cut" *49*

Table 10 - Chance detection results for different forest harvesting techniques *50*

Table 11 - Validation dataset summary for Bayts *69*

Table 12 - Change detection spatial and temporal assessment for NBR and NDVI time series, both for Bayts and BaytsDD. For BaytDD the monitoring period started in 2017, so the values for 2015 and 2016 were Not Available (NA). *71*

Table 13 - Simplified assessment for Bayts and BaytsDD using only "cut" and "no-cut" classes. *73*

Table 14 - Assessment for verifying the ability to detect changes due to different harvesting techniques. Since the BaytsDD was validated with a smaller validation dataset, only clear cut and coppice were in the dataset and hence for thinning and conversion the results were Not Available (NA). *73*

Table 15 - Sentinel-2 NDVI change detection results compared with results obtained using fractional cover time series from CLASlite. Sub-table: Upper for spatial accuracy, center for harvesting technique assessment, lower for spatial-temporal accuracy *83*

Table 16 - Comparison for spatial resolution increment in change detection algorithm using Sentinel-2 (10m), RapidEye (5m) and Planet Scope (3m) time series. Sub-table: Upper for spatial accuracy, center for harvesting technique assessment, lower for spatial-temporal accuracy *84*

List of equations

Eq. 1 – Intrinsic water use efficiency equation. *18*

Eq. 2 - Best Site Index model to explain ex-post fertility. *22*

Eq. 3 - Best Site Index model to predict the fertility ex-ante plantation *23*

Eq. 4 - Best simplified Site Index model to explain fertility without field survey *23*

Eq. 5 - Best model to explain the CAI in Douglas fir plantation. *25*

Eq. 6 - Best model to predict the CAI net *26*

Eq. 7 - Best diagnostic CAI model with simplified method. *26*

Eq. 8 - Normalized Burned Ration equation (on top), Normalized Difference Vegetation Index equation (on bottom). *45*

Eq. 9 - Normalized Burned Ratio equation with respective band number for Sentinel-2 products (on top), Normalized Difference Vegetation Index equation with respective band number for Sentinel-2 products (o bottom). *66*

Abstract

In a global changing framework forest importance is nowadays recognized and the awareness about sustainable practices and management is raising (European_Commission, 2013). As well as the needs of more knowledge and control on forest harvesting in Italian forest (Mori, 2019). Earth Observation science had an explosive growth since the policy change on data distribution for NASA Landsat archive (Wulder et al., 2012) and the advent of ESA Copernicus program. The access to these groundbreaking technologies leaded researcher to a different point of view in the forest sector. Immediately tropical forest deforestation drawn the majority of interests (Perbet et al., 2019; Tang et al., 2019; Shimizu et al., 2017; Reiche et al., 2013, 2016; Joshi et al., 2015; Asner et al., 2009), heading to the development of many different tools for tropical forest monitoring. This study was focused on the application of satellite remote sensing data (derived from Sentinel-2) to two cardinal aspect for Italian forest.

Since wood production plays a key role in developing a rural economy and stimulating the use of sustainable raw material, an increment of Douglas-fir plantation is desirable because of his great growth potential. Therefore, it was necessary to investigate good indices in order to assess the Douglas-fir land suitability and fertility indices. Empirical mathematical models were developed and validated using different sets of variables derived from remote sensing data and field survey. Models validation reached very good results for Site Index ranging from 0.63 to 0.97 R^2 and Current Annual Increment ranging from 0.50 to 0.98 R^2.

Furthermore, remote sensing data were applied to calibrate and validate different approaches for forest change detection. Knowing where and when forest harvests are done is crucial for correctly applying sustainable forest management and for controlling illegal logging. In this study was demonstrated that there are already tools developed in tropical forest that it could be applied to Italian forest. The best method was the basic one, which uses only summer images avoiding the seasonal noise problem in the time series but losing near-real time ability. If the temporal accuracy is essential the best method for removing time series seasonality resulted the harmonic model fitting, but further analyses are needed expanding the validation area in order to corroborate these results.

General Introduction

Forestry science and silviculture plays a key role in forest sustainability and forest carbon balance. In the previous centuries these factors were overwhelmed by the importance of forest production and the necessity of the population to growth. Nowadays, due to global warming and global change, forest managers awareness is raised on that and they are more focused on sustainable forest practices. This goal requires a comprehensive knowledge about the history and the future of forests.

In the last few decades, the technology advancement in computer science led to a massive improvement in modeling and prediction for the forest sector; the forest scientific research has benefited from this big step forward as well. This impressive progress has speed up the processing time and solved a large number of problems, nonetheless of course it has generated new ones. Generally, now in a research project focused on find relationships between variables, a major part of the study is spent to identify the really meaningful variables. This is because much more information and data are available now, but unexpectedly, this massive quantity of information can generate confusion and misinterpretation, not only benefits.

Meanwhile, the field of earth observation (EO) has seen explosive growth and development due to the large number of investments (public and private), as well as the aid from computer science progress (Ma et al., 2015; Prashanth, 2009). Therefore, the problems showed in the previous paragraph are present in the Earth Observation field as well. The number of planet images is growing, and the information carried by them are increasing even more due to sensors technology evolution.

1 Remote sensing: in general

The remote sensing is universally defined as the technique to measure surfaces or objects characteristics from a distance (Ma et al., 2015; Congalton, 1991) using many different tools which exploit different technology, more precisely:

"...remote sensing in the most generally accepted meaning refers to instrument-based techniques employed in the acquisition and measurement of spatially organized (most commonly, geographically distributed) data/information on some property(ies) (spectral; spatial; physical) of an array of target points (pixels) within the sensed scene that correspond to features, objects, and

materials, doing this by applying one or more recording devices not in physical, intimate contact with the item(s) under surveillance (thus at a finite distance from the observed target, in which the spatial arrangement is preserved); techniques involve amassing knowledge pertinent to the sensed scene (target) by utilizing electromagnetic radiation, force fields, or acoustic energy sensed by recording cameras, radiometers and scanners, lasers, radio frequency receivers, radar systems, sonar, thermal devices, sound detectors, seismographs, magnetometers, gravimeters, scintillometers, and other instruments" (Short, 2009).

Beside this comprehensive definition of general remote sensing, when the focus is earth observation (EO), the remote sensing is often based on electromagnetic radiation, mainly visible and infrared spectrum. Thus, the data are values of reflected or emitted energy from a surface or an object (Prashanth, 2009). The electromagnetic radiation range is very wide, an overview of the range variation is given in the Figure .

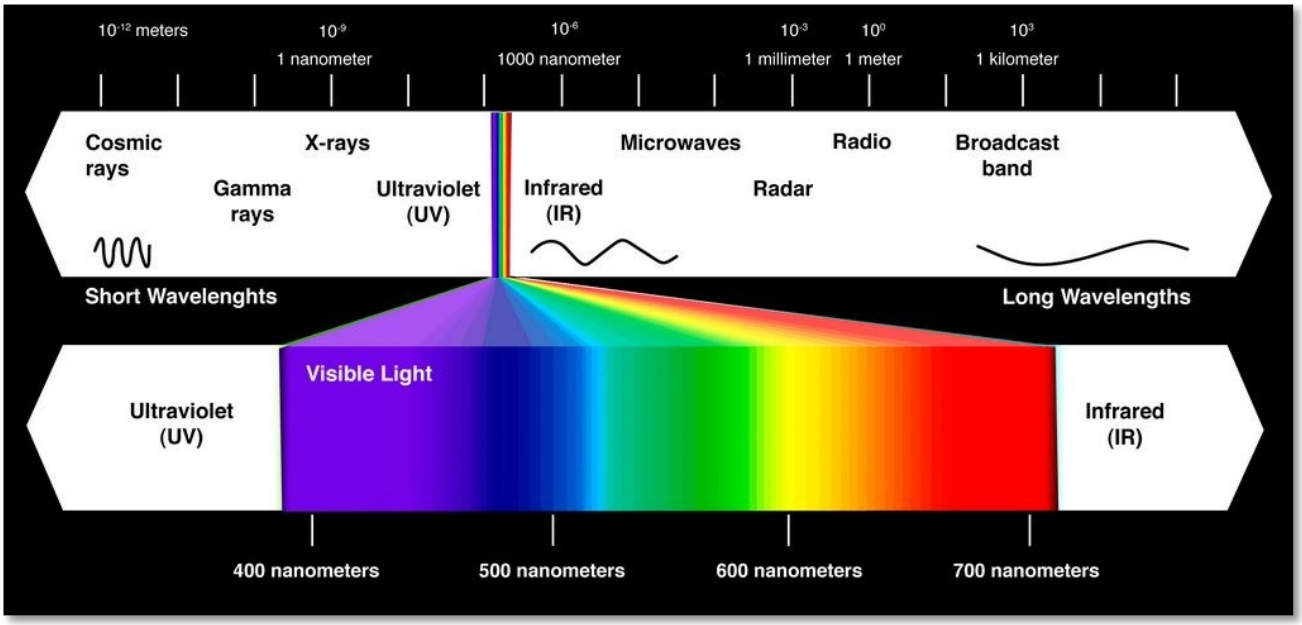

Figure 1 - Electromagnetic spectrum (Mukesh, 2015). Visible, infrared and microwave are currently the most relevant ranges used in earth observation.

The ability of Remote Sensing to measure physical characteristic of real object without relying on physical contact it's essential for the study of our planet. Indeed, it's already broadly used in a large number of applications, such as agriculture, forestry, urban planning, disaster monitoring, etc. (Zanetti, 2017). This different fields of application are possible only because the Earth Observation is made by different sensors, which measures different object characteristics.

Some of the most common sensors are called passive, it measures the reflected sunlight, or the direct energy emitted from the earth surface in the visible and near- to middle infrared range of wavelength. Alternatively, some sensors measures the backscatter from surface of the energy emitted from the sensor vehicle itself and they are called active sensor, such as laser or radar (Richards and Jia, 2013; Prashanth, 2009).

Different platforms are used to carried out Remote Sensing imaging, for example drones, aircraft and spacecraft. The sensors are mostly similar, but the difference in their distance from the earth and stability can lead to different image properties, especially in spatial resolution. The spacecraft platforms are divided in two classes based mainly on their altitude: low earth orbiting and geostationary. In the first class the satellites orbit is usually sun-synchronous, that means that the images acquisition is made at the same local time in each orbit, thus are used mainly for earth surface and oceanographic observations. The geostationary satellites are higher in elevation and, even if the imaging technology is similar to the low earth orbiting satellites, the images spatial resolution are much lower, therefore are generally used for weather and climate studies (Richards and Jia, 2013).

The manned airplanes were the first carrier for remote sensing sensors but in the last 15 years the novelty of the drones it became more significant. For local investigation the drone is unbeatable in terms of precision: the images has ultra-high spatial resolution with a ground spacing in centimeter-level as well as the geolocation accuracy (Surový et al., 2019). However, the problems of the drones are the relative high costs for the survey, this is big constraint regard to the temporal resolution, and the limitation of the survey extension making impossible to do global and nation wise study.

2 Sources of errors

Taking photos from the space is not as easy as it sounds like. In fact, remote sensing images must to be corrected before use in studies and research. The main errors are classified in two categories: radiometric errors and geometric errors.

The latter one is originated from several issues. The relative motions of the satellite and the earth, the non-idealities in the sensor, the curvature of the earth, the variations of attitude, velocity and position of the platforms can all lead to different geometric errors. Usually these errors can be corrected exploiting models of the source of errors, this process is explained in detail by Richards and Jia (2013).

The radiometric errors, i.e. errors of the pixels brightness, are mainly due to the interaction of the solar radiation with the atmosphere compounds and noise in the electronics sensor components (Prashanth, 2009). As the geometric errors, there are several ways to overcome these errors and usually they are corrected from the agency/owner of the images before releasing them. For instance, the European Space Agency for the Sentinel-2 images provide different level of products with different level of correction: from only the strictly needed to almost all the correction mentioned in the previous paragraphs (SUHET, 2015).

For advanced analysis using multitemporal images, as time series analysis, another problem should be considered. The misregistration for the same tile acquired in different time, indeed the geolocation accuracy is far from the perfection and this lead to difficulties and errors during multitemporal analysis especially for change detection (Roy, 2000). Sentinel-2 images has a very high geolocation accuracy but this problem still raising awareness in the scientific community, although the mean error was estimated to 0.4 10m pixel (Yan et al., 2018).

3 Concept of resolution

It's possible to distinguish between three kinds of resolutions: *spatial, spectral and temporal resolution*.

The *spatial resolution* is equivalent to the minimum spatial unit on the ground and it's represented by the pixel size. The remote sensing image is a grid of pixels obtained by continuous ground scanning. The energy (photons), within this spatial unit, coming from different objects is averaged (Prashanth, 2009).

Each sensor is built to work in combination to prisms and spectral filters, which are able to split the electromagnetic spectrum in sectors and aggregate the energy for each band wavelengths. The wavelength interval characterizes the *spectral resolution* for the visible/infra-red sensors. A high spectral resolution image corresponds to a high number of bands with a narrow width, on the other hand, a lower number of bands correspond to a wider band width. The number of bands in the image effect the ability of the sensor to distinguish different sensed materials, the more are the number of bands the better is the chance to discriminate different materials (Prashanth, 2009).

The *temporal resolution* is the frequency of revisit time for the same location on the ground, in other words, the time between each satellite passage. This characteristic is crucial for some applications in monitoring and change detection.

4 Remote sensing applied to forest management

Recently the forestry sector is more aware of the remote sensing potentials regardless the carriers. Nowadays several opportunities for improving decision support and inventories are coming from satellites, aircrafts and drones. Every platform can carry similar sensor but usually they differ for spatial and spectral resolution in the images due to different altitude during the survey. However, the forest managers chose the remote sensing source based on the goal to be accomplished and the extension of the area to be assessed.

Knowing the current state and the temporal dynamics of the forest is crucial for both forest management and forest policy (Kennedy et al., 2007). Today, one of the most important challenge is the estimation of nationwide carbon balance in order to follow the goals and guidelines from REDD+. Since the forest is one of the key parts for their carbon stock, one affordable way to address this challenge is provided by remotely sensed data which has the potential to assess current and historical tendencies of forest degradation and deforestation (James Baker et al., 2010).

As the carbon stock estimation, the demands for nationwide forest inventories continue to increase but the financial resources dedicated to that purpose are diminishing (White et al., 2016). In this context remote sensing technology will gain importance due to their ability of measuring some direct information or deriving others data by modelling (Brosofske et al., 2014). The more relevant technologies for inventories purpose and thus, those more studied by the scientific community include: high and very-high spatial resolution (HSR and VHSR) satellite optical imagery, digital aerial photogrammetry (DAP), airborne laser scanning (ALS) and terrestrial laser scanning (TLS) (White et al., 2016).

One of the greatest advantages of remote sensing is the possibility to cover the entire globe multiple times, and now reaching a new global coverage almost every day with useful information about the forest. Therefore, a forest global monitoring is affordable and precise for many applications. Surely, monitoring illegal logging and deforestation in the tropical forests are the leading purposes in the monitoring field (Shimizu et al., 2017; Joshi et al., 2015; Hansen et al., 2013; Verbesselt et al., 2012; Asner et al., 2009).

More interesting to the enterprise-level forest managers are the structural and spectral properties of the forest. Remote sensing data are broadly used to estimate structural parameters, such as: strata and zones of the forests, detection regeneration, canopy height estimation, diameter or basal area, canopy closure, etc. Although, the spectral information is related to the chemical compounds

in the canopy and leaf, this lead to more complex assessment for example tree species classifications and forest health assessment (Surový et al., 2019).

5 Aims of the thesis

Accordingly on what mentioned in the previous paragraphs and scientific literature, the remote sensing is leading a revolution in the forestry sector, either on scientific research and operational level (Surový et al., 2019; Noorian et al., 2016). The impact of this technology is highly effective in several aspects, we have chosen two quite different applications in order to response at current issues in the Italian forest sector. The forest is crucial for carbon stock, climate change mitigation and biodiversity conservation (Dinerstein et al., 2019), this is remarkably true for tropical forest but European and Italian forest are not less important.

In the Chapter I the use of remote sensing was applied in combinations with numerous other environmental characteristics to evaluate the best sets of variables in order to estimate Douglas-fir fertility indices. The Douglas-fir (*Pseudotzuga menziesii* (Mirb.) Franco) in Italy can be used to help rural economy because of his ability to outproduce native coniferous and broadleaf (Lavender and Hermann, 2014; Ciancio et al., 1980) in terms of wood production. In order to reach this goal, the Douglas-fir plantation has to be expanded and thus reliable fertility indices and land suitability indicators are necessary for both planning and managing the plantations. The Site Index as the most common productivity and site quality indicator (Bueis et al., 2016; Corona et al., 1998) was investigated in conjunctions with the current annual increment ad fixed age (proposed as new fertility indicator).

Since 2015 the Italian statistical institute (ISTAT) has stopped to collect and publish data about the real volume and forest surface harvested in Italy. This lack of information is due to a fractionated system of forest management and control to regional and province level. Usually the logging authorization released from the authority are not strict about the timing of operation and allow the logger to cut less than what he requested. This permissibility and the control deficiency, led to a not reliable data, i.e. the administrative data are useless for harvesting statistics. The Italian national forest report 2017-2018 has highlighted this problem, because a carefully designed planning on the growing and harvesting rate is essential for the sustainability of the forest sector. For this purpose, the remote sensing is a suitable solution because of the large number of freely available data and a relatively high spatial and temporal resolution. The Chapter II and Chapter III are focused on assessing the possibility to use different monitoring techniques developed for tropical forest in

Italian one. These studies try to evaluate and overcame difficulties due to several aspects such as the seasonality in the forest, different logging practices (e.g. coppice, thinning, transformation to high forest, etc), varying terrain topography and different forest reaction to harvest. In this context some scientific methodologies were assessed and evaluated with the aim of nationwide estimation of forest harvest/disturbance.

In the Chapter II, a Bayesian approach for forest change detection developed by Reiche et.al (2015a) was used. In this chapter many difficulties and problems were avoided using a simplified method: Sentinel-2 derived indices (NBR, NDVI) were calculated from a summer only time series. In this condition the seasonality was excluded, but the time series utilized were only partial and not along all year.

In the Chapter III, the whole Sentinel-2 time series was used, and two method to overcome the seasonality were assessed. Firstly, the previous approach was adopted with a spatial normalization proposed by the author to reduce the seasonality effect (Reiche et al., 2018a), after that, a more advanced algorithm with seasonality harmonic model fitting option was tested (Reiche et al., 2018b).

Finally, in the Chapter IV, the simplified method was employed to evaluate different time series, i.e. the fractional cover derived from the software CLASlite (Asner et al., 2009), gaining information from the whole spectral signature. Moreover, time series with different spatial resolution from 10m (Sentinel-2), 5m (RapidEye), and 3m (PlanetScope) were studied in order to verify if an increasing spatial resolution lead to an increasing accuracy.

5.1 How to read the thesis

The thesis main part is composed by 3 consecutive chapters, each one explains in detail problems and applications of remote sensing to forest monitoring and management. All chapters are organized as independent scientific paper, with a proper Introduction, Materials and Methods, Result, Discussion and Conclusion sections. The thesis ends with a General Conclusion chapter, that encloses a general explanation of the achievements and knowledge increases due to this work.

6 Bibliography

Asner, G.P., Knapp, D.E., Balaji, A., Páez-acosta, G., 2009. Automated mapping of tropical deforestation and forest degradation : CLASlite. J. Appl. Remote Sens. 3, 1–24. doi:10.1117/1.3223675

Brosofske, K.D., Froese, R.E., Falkowski, M.J., Banskota, A., 2014. A Review of Methods for Mapping and Prediction of Inventory Attributes for Operational Forest Management. For. Sci. 60, 733–756. doi:10.5849/forsci.12-134

Bueis, T., Bravo, F., Pando, V., Turrión, M., 2016. Relationship between environmental parameters and Pinus sylvestris L. site index in forest plantations in northern Spain acidic plateau. iForest - Biogeosciences For. 008, e1–e8. doi:10.3832/ifor1600-008

Ciancio, O., Eccher, A., Gemignani, G., 1980. Eucalitti, pino insigne, douglasia ed altre specie a rapido accrescimento. Ital. Agric. 117, 190–214.

Congalton, R.G., 1991. A review of assessing the accuracy of classifications of remotely sensed data. Remote Sens. Environ. 37, 35–46. doi:10.1016/0034-4257(91)90048-B

Corona, P., Scotti, R., Tarchiani, N., 1998. Relationship between environmental factors and site index in Douglas-fir plantations in central Italy. For. Ecol. Manage. 110, 195–207. doi:10.1016/S0378-1127(98)00281-3

Dinerstein, E., Vynne, C., Sala, E., Joshi, A.R., Fernando, S., Lovejoy, T.E., Mayorga, J., Olson, D., Asner, G.P., Baillie, J.E.M., Burgess, N.D., Burkart, K., Noss, R.F., Zhang, Y.P., Baccini, A., Birch, T., Hahn, N., Joppa, L.N., Wikramanayake, E., 2019. A Global Deal For Nature: Guiding principles, milestones, and targets. Sci. Adv. 5, eaaw2869. doi:10.1126/sciadv.aaw2869

European_Commission, 2013. A new EU Forest Strategy: for forests and the forest-based sector. Brussels.

Hansen, M.C., Potapov, P. V., Moore, R., Hancher, M., Turubanova, S.A., Tyukavina, A., Thau, D., Stehman, S. V., Goetz, S.J., Loveland, T.R., Kommareddy, A., Egorov, A., Chini, L., Justice, C.O.,

Townshend, J.R.G., 2013. High-Resolution Global Maps of 21st-Century Forest Cover Change. Science (80-.). 342, 850–853. doi:10.1126/science.1244693

James Baker, D., Richards, G., Grainger, A., Gonzalez, P., Brown, S., Defries, R., Held, A., Kellndorfer, J., Ndunda, P., Ojima, D., Skrovseth, E., Souza, C.L., Stolle, F., Baker, D.J., 2010. Achieving forest carbon information with higher certainty: A five-part plan. Environ. s cience p olicy 13, 249–260. doi:10.1016/j.envsci.2010.03.004

Joshi, N., Mitchard, E.T.A., Woo, N., Torres, J., Moll-Rocek, J., Ehammer, A., Collins, M., Jepsen, M.R., Fensholt, R., 2015. Mapping dynamics of deforestation and forest degradation in tropical forests using radar satellite data. Environ. Res. Lett. 10. doi:10.1088/1748-9326/10/3/034014

Kennedy, R.E., Cohen, W.B., Schroeder, T.A., 2007. Trajectory-based change detection for automated characterization of forest disturbance dynamics. Remote Sens. Environ. 110, 370–386. doi:10.1016/j.rse.2007.03.010

Lavender, D.P., Hermann, R.K., 2014. Douglas-fir: The Genus Pseudotsuga. Oregon State University, Corvallis, OR.

Ma, Y., Wu, H., Wang, L., Huang, B., Ranjan, R., Zomaya, A., Jie, W., 2015. Remote sensing big data computing: Challenges and opportunities. Futur. Gener. Comput. Syst. doi:10.1016/j.future.2014.10.029

Mori, P., 2019. Statistiche forestali: Potenzialità e opportunità per ripartire da zero. Sherwood - For. ed alberi oggi 13–15. doi:ISSN 1590-7805

Mukesh, K., 2015. How does remote sensing utilize electromagnetic radiation? [WWW Document]. Quora. URL https://www.quora.com/How-useful-is-the-electromagnetic-spectrum-to-remote-sensing

Noorian, N., Shataee-Jouibary, S., Mohammadi, J., 2016. Assessment of different remote sensing data for forest structural attributes estimation in the Hyrcanian forests. For. Syst. 25. doi:10.5424/fs/2016253-08682

Perbet, P., Fortin, M., Ville, A., Béland, M., 2019. Near real-time deforestation detection in Malaysia and Indonesia using change vector analysis with three sensors. Int. J. Remote Sens. 40, 7439–7458. doi:10.1080/01431161.2019.1579390

Prashanth, R.M., 2009. Geographic Object-based Image Analysis. Bergakademie Freiberg.

Reiche, J., de Bruin, S., Hoekman, D.H., Verbesselt, J., Herold, M., 2015. A Bayesian approach to combine landsat and ALOS PALSAR time series for near real-time deforestation detection. Remote Sens. 7, 4973–4996. doi:10.3390/rs70504973

Reiche, J., Hamunyela, E., Verbesselt, J., Hoekman, D., Herold, M., 2018a. Improving near-real time deforestation monitoring in tropical dry forests by combining dense Sentinel-1 time series with Landsat and ALOS-2 PALSAR-2. Remote Sens. Environ. 204, 147–161. doi:10.1016/j.rse.2017.10.034

Reiche, J., Lucas, R., Mitchell, A.L., Verbesselt, J., Hoekman, D.H., Haarpaintner, J., Kellndorfer, J.M., Rosenqvist, A., Lehmann, E.A., Woodcock, C.E., Seifert, F.M., Herold, M., 2016. Combining satellite data for better tropical forest monitoring. Nat. Clim. Chang. 6, 120–122. doi:10.1038/nclimate2919

Reiche, J., Souza, C.M., Hoekman, D.H., Verbesselt, J., Persaud, H., Herold, M., 2013. Feature Level Fusion of Multi-Temporal ALOS PALSAR and Landsat Data for Mapping and Monitoring of Tropical Deforestation and Forest Degradation. IEEE J. Sel. Top. Appl. Earth Obs. Remote Sens. 6, 2159–2173. doi:10.1109/JSTARS.2013.2245101

Reiche, J., Verhoeven, R., Verbesselt, J., Hamunyela, E., Wielaard, N., Herold, M., 2018b. Characterizing Tropical Forest Cover Loss Using Dense Sentinel-1 Data and Active Fire Alerts. Remote Sens. 2018, Vol. 10, Page 777 10, 777. doi:10.3390/RS10050777

Richards, J.A., Jia, X., 2013. Remote Sensing Digital Image Analysis, Fifth edit. ed, Remote Sensing Digital Image Analysis. Springer Heidelberg, New York, Dordrecht, London. doi:10.1007/978-3-662-03978-6

Roy, D.P., 2000. The impact of misregistration upon composited wide field of view satellite data and

implications for change detection. IEEE Trans. Geosci. Remote Sens. 38, 2017–2032. doi:10.1109/36.851783

Shimizu, K., Ponce-Hernandez, R., Ahmed, O.S., Ota, T., Chi Win, Z., Mizoue, N., Yoshida, S., 2017. Using Landsat time series imagery to detect forest disturbance in selectively logged tropical forests in Myanmar. Can. J. For. Res. 47, 289–296. doi:10.1139/cjfr-2016-0244

Short, N.M., 2009. NASA Remote sensing tutorial [WWW Document]. NASA. URL http://rst.gsfc.nasa.gov

SUHET, 2015. SENTINEL-2 User Handbook. doi:GMES-S1OP-EOPG-TN-13-0001

Surový, P., Kuželka, K., Surový, P., Kuželka, K., 2019. Acquisition of Forest Attributes for Decision Support at the Forest Enterprise Level Using Remote-Sensing Techniques—A Review. Forests 10, 273. doi:10.3390/f10030273

Tang, X., Bullock, E.L., Olofsson, P., Estel, S., Woodcock, C.E., 2019. Near real-time monitoring of tropical forest disturbance: New algorithms and assessment framework. Remote Sens. Environ. 224, 202–218. doi:10.1016/J.RSE.2019.02.003

Verbesselt, J., Zeileis, A., Herold, M., 2012. Near real-time disturbance detection using satellite image time series. Remote Sens. Environ. 123, 98–108. doi:10.1016/J.RSE.2012.02.022

White, J.C., Coops, N.C., Wulder, M.A., Vastaranta, M., Hilker, T., Tompalski, P., 2016. Remote Sensing Technologies for Enhancing Forest Inventories: A Review. Can. J. Remote Sens. 42, 619–641. doi:10.1080/07038992.2016.1207484

Wulder, M.A., Masek, J.G., Cohen, W.B., Loveland, T.R., Woodcock, C.E., 2012. Opening the archive: How free data has enabled the science and monitoring promise of Landsat. Remote Sens. Environ. 122, 2–10. doi:10.1016/j.rse.2012.01.010

Yan, L., Roy, D.P., Li, Z., Zhang, H.K., Huang, H., 2018. Sentinel-2A multi-temporal misregistration characterization and an orbit-based sub-pixel registration methodology. Remote Sens. Environ. 215, 495–506. doi:10.1016/j.rse.2018.04.021

Zanetti, M., 2017. Advanced methods for the analysis of multispectral and multitemporal remote sensing images. Thesis. University of Trento.

Chapter I – Site Index and growth prediction from remote sensing and environmental factors in Douglas-fir plantations

1 Abstract

The Italian Douglas-fir plantations (10 000 ha) are not widespread as in nearby European states, France (333 000 ha) as well as Germany (100 000 ha) (Lavender and Hermann, 2014). However the Douglas-fir plantations in Italy are able to outproduce both native conifers and broadleaves (Lavender and Hermann, 2014; Ciancio et al., 1980) in terms of wood production.

Since wood production plays a key role in developing a rural economy, an increment of Douglas-fir plantation is essential in order to achieve this objective. Therefore, it is necessary to investigate good indices in order to assess the Douglas-fir land suitability.

In this study two fertility indices, Site Index at 50 years old and net current annual increment, were adopted with the aim of finding their relationships with environmental characteristics, such as climate, soil and biochemical factors together with some remote sensed indices.

The assessment plots were located in public property plantations. They differed in structure (density and volume), climate and soil characteristics, but they were similar in tree age.

The statistical analysis was based on empirical mathematical models (multiple linear regression). Akaike information criterion (AIC) was implemented in order to select the most relevant subset of variables, then five best models for each fertility index were validated with Leave-One-Out Cross-Validation (LOOCV) to identify the best prediction model.

Each fertility index was studied to obtain both prognostic and diagnostic predictions. For these purpose different subsets of variables were selected; in the prognostic model only variables not directly related to stand were used while in the diagnostic model there were adopted all the variables. Moreover, a further simplified diagnostic model was elaborated using the variables which did not need field survey.

Both fertility indices were related to the variables; the majority of variance was explained by the diagnostic models (site index R^2 = 0.97; CAI R^2 = 0.98), differently, the prognostic models reached the worst results with the lower explained variance (site index R^2 = 0.63; CAI R^2 = 0.50) and the simplified approach got mid-way results (site index R^2 = 0.75; CAI R^2 = 0.56).

2 Introduction

Douglas-fir (*Pseudotsuga menziesii* (Mirb.) Franco) was introduced in Italy since the end of XIX century during significant reforestation programs focused on wood production aims.

Nowadays, it is possible to find its plantations in most Italian regions, nevertheless the main planting areas are located in the central part of the peninsula, such as in Tuscany and Emilia Romagna. Moreover, after a century of studies and tests, several authors shown that the Douglas-fir growth rate makes possible to outproduce both native conifers and broadleaves (Lavender and Hermann, 2014; Corona et al., 1998; Ciancio et al., 1980) and they have proposed Apennines as its optimal vegetation zone (Lavender and Hermann, 2014; Corona et al., 1998). Furthermore, no serious disease were observed (Corona et al., 1998; Ciancio et al., 1981) and a more recent study has shown substantial improvement on soil C sequestration, N stock and microbial activity rather to indigenous beech forest (Antisari et al., 2015).

However, the plantation extension in Italy (10 000 ha) are far less than the nearby European state, such as France (330 000 ha) and Germany (100 000 ha) (Lavender and Hermann, 2014).

In this context, an increment of Douglas-fir plantation it is possible and useful for developing a stronger rural economy.

For those reasons reliable fertility indices and land suitability indicators are necessary for both planning and managing plantations. In fact, lots of authors were focused on finding relationship between productivity indices and site features, such as soil, climate and topographic characteristics (Littke et al., 2016; Kimsey et al., 2008; Curt et al., 2001; Corona et al., 1998); despite all of these efforts, they were able to reach just low amount of explained variance (R^2= 0.4 - 0.58), except for Littke et al. (2016) which has got R^2=0.89 during calibration and R^2=0.66 on validation but using boosted regression trees (BRT) models.

The aim of this investigation was to develop multiple linear regression models in order to explain and predict important information for forest planning and management such as Site Index and stand growth rate (net current annual increment). The fist one it is the most common site quality and productivity indicator (Bueis et al., 2016; Corona et al., 1998) and the second one was proposed as fertility index since it was used at fixed age.

This purpose was achieved with three different sets of variables to simulate different level of data availability and distinguish between prognostic (ex-ante) and diagnostic (ex-post) models.

3 Materials and methods

3.1 Study area

The study was carried out in *P. menziesii* plantations inside the Foreste Casentinesi National Park, located in Italian Northern Apennine (Figure 2). The climate region is warm temperate, occasionally, with short summer drought; the rainiest periods are Autumn and Spring and in winter the snow cover is common.

The soils are sandy-loam and sometimes clay-loam, with normal LFH horizon due to their agriculture history.

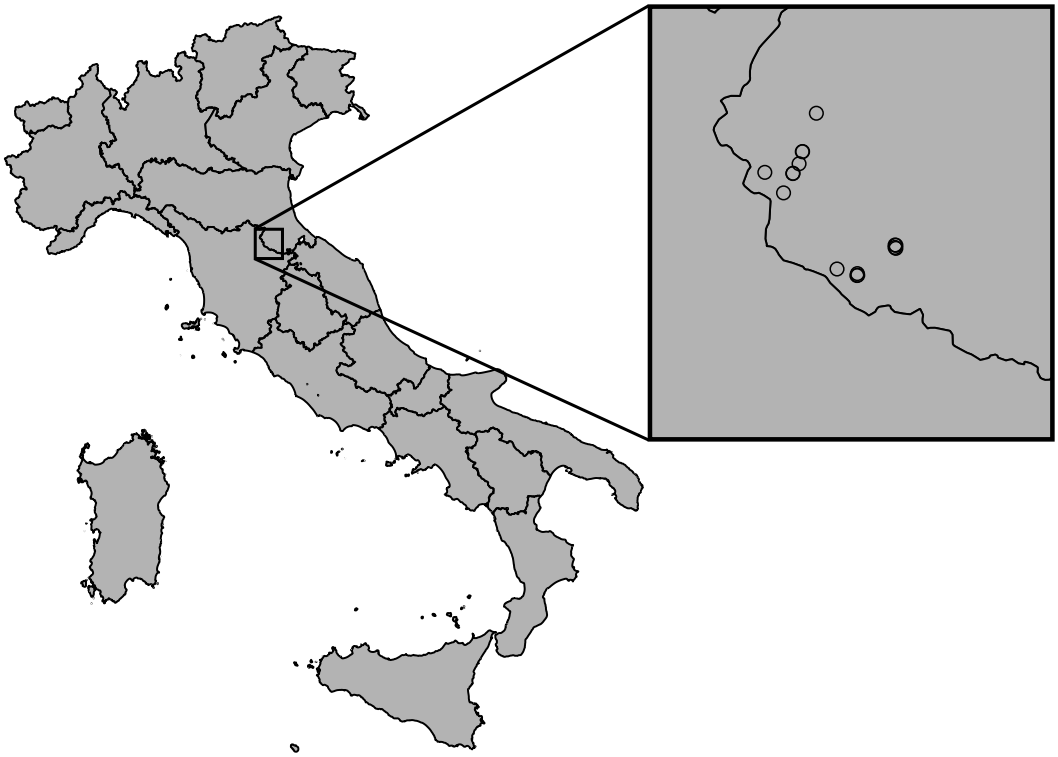

Figure 2 - Location of the study area and relative plots for field survey.

Fifteen field plots with approximately the same stand age were chosen, in order to cover a wide range of elevation, local climate and stands structure (density and volume; see Table 1). The stands were situated between 530 and 825 m a.s.l., with slopes range between 5 and 60% and they were even-aged plantations on ex-agricultural land; stands with a known history of thinning, fire or storm disturbance during the reference study-period (2003 - 2015) were excluded from the analysis.

3.2 Stands data

A square 30 m plot was permanently located in each stand, and the all trees measurement were repeated in two date, 2003 and 2015. All heights were interpolated by a species-specific model (Curtis, 1967) in order to reduce the uncertainty associated with height measurement. Initially it was calibrated with data from both survey date and for each plot, then the heights were predicted as function of tree age and diameter at breast height (DBH).

Stem volume was estimated for each date as a function of tree height and diameter using a site-specific allometric model (Bernetti, 1965), corrected for treetop volumes. Then, stand net current annual increments (CAI) were estimated as volumes cumulated difference in 2015 and 2003.

In order to correct for small age differences among stands, a species-specific top height model (Maetzke and Nocentini, 1994) was used to estimate the Site Index (mean height of the 100 dominant thickest trees per hectare at age of 50 years) for every plot as a function of top height and age.

Table 1 - Measured and estimated stands characteristics (value between all 15 plots).

	Max	**Min**	**SD**
Age years	48	40	3
Density trees/ha	933	511	119
DBH (mean) cm	38	28	3
H (mean) m	29	23	2
Hd m	36	27	3
SI m	38	31	2
Volume m^3ha^{-1}	928	541	114
CAI net $m^3ha^{-1}years^{-1}$	27.7	7.5	6.6

Note: *To be notice the plots heterogeneity in terms of volume and density as well as current annual increment and the relatively homogeneous stands age.*

3.3 Soil variables

For each stand, soil samples were taken in center of the plot, as well in all four cardinal directions with 10 m distance from plot center. For each sampling point, the samples were taken at three different depths, corresponding to the forest floor (LFH), superficial (0-10 cm) and bulk mineral soil (25-35 cm).

In the laboratory, the samples were air-dried, manually grounded and sieved to 2 mm in order to remove rocks and roots. Soil texture at both depths was assessed by standard laboratory methods (Kettler et al., 2001) modified with 20 min sedimentation time.

Small sub-samples were weighted in silver capsules and scanned by an elemental analyzer CHNS-O (mod. Flash 2000, Thermo Scientific, MA) connected online to the isotope mass spectrometer (DELTA V Advantage, Thermo Scientific, MA) in order to estimate biochemical indices (soil C/N ratio, soil $\boldsymbol{\delta}^{15}$N and forest floor $\boldsymbol{\delta}^{13}$C). The small soil samples were pretreated before the elemental analyzer with HCl 6M to remove all the carbonates. Soil $\boldsymbol{\delta}^{15}$N value was estimated as an index of N availability and net nitrification (Kahmen et al., 2008; Templer et al., 2007).

Forest floor $\boldsymbol{\delta}^{13}$C was measured as water stress index (Wilson and Maouire, 2009; Ehleringer et al., 2002; O'Leary, 1993; Farquhar et al., 1982), neglecting any effects of fractionation during decomposition. Intrinsic water use efficiency (iWUE) was estimated from $\boldsymbol{\delta}^{13}$C (Leonardi et al., 2012; Farquhar et al., 1989):

$$iWUE = 0.625\ C_a\left(1 - \frac{\Delta^{13}C - a}{b - a}\right)$$

Eq. 1 – Intrinsic water use efficiency equation.

Reference values of atmospheric $\boldsymbol{\delta}^{13}$C and CO_2 concentration were derived from the literature (Dlugokencky et al., 2016; White et al., 2015).

3.4 Climatic variables

Climatic variables for each plot could not be measured directly, but they were estimated from a dense network of nearby meteorological stations which are managed by Regional Meteorological Service (ARPAE) and water utility company (Romagna Acque S.p.A.). Monthly temperature and precipitation data in the period 2003-2015 were used. Mean, minimum and maximum temperatures

from the nearest meteorological station were corrected for each field plot. The data error was due to different elevation between field plot and meteorological station, so a monthly lapse rate was used. It was computed over the entire study area using the entire stations network (between 41 and 1060 m a.s.l).

A similar error for monthly precipitation data was corrected, this error was due to the distance between filed plots and nearest meteorological station. Long-term correction factors, based on available precipitation maps (1961/1999), were used.

According to Rehfeldt et al. (2014), a suite of climate variables statistically related to *P. menziesii* climate niche was computed for each plot (see Table 2).

Table 2 - Climate variable statistically relevant to delineate Douglas-fir niche according to Rehfeldt et al. (2014)

Variable	Unit	Definition
MTCM	°C	Mean temperature in the coldest month
MTWM	°C	Mean temperature in the warmest month
MMAX	°C	Maximum temperature in the warmest month
SUMP	mm	Sum of July and August precipitation
TDIFF	°C	Summer–winter temperature differential: MTWM - MTCM

Note: *abbreviation used along the article and how were computed the variables with their units.*

Since the great importance of site water balance demonstrated for *P. menziesii* growth (Corona et al., 1998; Tyler et al., 1996), the annual sum of soil water deficit and surplus were computed for each plot as Thornthwaite and Mather (1957) suggested. The USGS tool available online (McCabe and Markstrom, 2007) was applied.

Solar radiation values for each plot were extracted from the Climate-SAF database (Huld et al., 2012; Šúri et al., 2007), correcting for plot slope and aspect.

3.5 Remote sensed variables

Lastly, the set of variables was completed with six remotely sensed indices, which are related to Net Primary Production (NPP), photosynthetic activity, chlorophyll content and leaf nitrogen (Xiao et al., 2018; Weiss and Baret, 2016; Dash and Curran, 2004; Gower et al., 1999): the Fraction of Absorbed

Photosynthetically Active Radiation (FAPAR), Leaf Area Index (LAI), Canopy chlorophyll content (Cab), MERIS terrestrial chlorophyll index (MTCI), Inflection Point in the Red Edge (REIP).

Due to the high spatial resolution of Sentinel-2 images, S-2 products were choosing to compute the remotely sensed variables. The Level 1C (top-of-atmosphere radiance) product was downloaded from Copernicus Open Access Hub web site, after a quick look at the products, the image with sensing date 2015/07/04 was selected in order to match the field survey period and exclude the clouds problem. The process to Level 2A (top-of-canopy reflectance) product was done by SNAP v6.0 software and the internal plug-in sen2cor (Müller-Wilm, 2017) with setting as default and the terrain correction with Digital Elevation Model from the Shuttle Radar Topography Mission enabled.

Afterward, the indices were calculated using SNAP functions within thematic land and biophysical processor. Lastly remote sensed variables were extracted from the grids (10x10 pixel resolution) for each plot calculating mean over the plots area.

3.6 Models development

The relationship between each dependent variable (CAI and SI) and potential predictors was assessed through a sequential process of model calibration and validation, which was entirely executed in the open source software R (R_Core_team, 2016).

Firstly, three subsets of variables were selected in order to simulate different variables availability and distinguish the models potential. The prognostic models were developed without variables directly related to stands aimed at predicting the fertility indices ex-ante the Douglas-fir plantation. The diagnostic models were developed with all variables to reach the best possible variance explanation. Lastly, simplified diagnostic models were proposed selecting just the variables which did not need field survey.

Based on information theory (IT), the most reliable multiple linear regression models were determined by the Akaike Information Criterion (AIC) through an iterative comparison of all possible variables combinations (Aertsen et al., 2010; Zuur et al., 2007), using the glmulti::glmulti R function.

Therefore, five best models resulting from each AICc screening were selected and compared through a calibration (bootstrap) and validation process. Model validation on an independent dataset is recognized as the most effective way to assess model reliability (Amaro et al., 2015). The validation process was based on the Leave-One-Out-Cross-Validation (LOOCV) method and

executed through the *caret*::*train* R function (Aertsen et al., 2010): the model was fitted to 14 plots values and the 15th plot was predicted by that model, afterwards the prediction result from the model and the real values of 15th plot was compared. This procedure was repeated for 15 times and every time using different plot as 15th one.

The predictive performance of each model was quantified in terms of explained variance fractions (R^2) (Aertsen et al., 2010), model root mean square error (RMSE), which is the absolute goodness-of-fit indicator and describes the difference between observed and predicted values in measurement units (Aertsen et al., 2010). Lastly, the relative root mean square error (RMSE%) was used to add more information on models assessment.

Table 3 - Input variables list.

Variables	Unit	Max	Min	SD
Altitude	m a.s.l.	825	199	153.9
Slope	%	60	5	0.2
Sand_10	%	41	12	9.4
Clay_10	%	12	5	1.8
Sand_35	%	38	11	8.4
Clay_35	%	16	5	3.1
C/N_litter	-	42.6	25.9	4.2
C/N_10	-	13.6	9.2	1.4
C/N_35	-	9.0	6.8	0.6
δ^{15}N _10	‰	2.1	-1.5	1.0
δ^{15}N _35	‰	3.4	1.0	0.8
WUEi	-	99.2	77.2	5.6
Volume (V)	m^3/ha	927.6	541.4	114.3
Age	years	48	40	2.5
MMAX	°C	30	25.8	1.3
MTWM	°C	23.1	20.1	1.0
MTCM	°C	3.5	1.9	0.4
TDIFF	°C	19.6	17.6	0.8
SUMP	mm	139	98	12.6
Rad	kWh	192	128	17.5
Sum_deficit	mm	75	26	16.0
Sum_surplus	mm	1194	426	259.8
LAI	-	3.1	2.5	0.212
FAPAR	-	0.77	0.69	0.027
Cab	-	193	132	17.5
MTCI	-	5.3	3.7	0.396
REIP	-	723	721	0.718
NDVI	-	0.86	0.82	0.01

4 Results

4.1 Site Index

The five best models ranked by AICc were selected, despite the significance threshold of two AICc units according to Calcagno and Mazancourt (2010). These models were calibrated with bootstrap and validated with LOOCV.

The coefficients of determination (R^2) computed in validation and calibration did not corroborated the AICc ranking, see Table 4.

As expected, the $SI_{ex\text{-}post}$ analysis achieved the best prediction results up to R^2 = 0.97 and RMSE = 0.36 m in the validation step using the following model:

$$SI_{ex-post} = 117.59 + (0.84\ MMAX) - (4.26\ TDIFF) + (0.26\ Cab) - (29.06\ LAI) + (0.2\ Sand\_10) + (0.06\ Rad) - (3.02\ Slope)$$

Eq. 2 - Best Site Index model to explain ex-post fertility.

All five $SI_{ex\text{-}post}$ models agreed with the importance of MMAX and TDIFF variables and even Cab and LAI were often selected by AICc. Regardless the different variables selected, the results were quite similar in terms of R^2 and RMSE.

$SI_{ex\text{-}ante}$ models selection were much more uniform, since all the five models agreed with the importance of CN_35, MMAX and MTWM, furthermore the relative importance of predictors were confirmed by *calc.relimp::relaimpo* function (R) according to Chevan and Southerland (1991); each model was based on these three variables plus one (Table 4).

Table 4 - Site Index models summary.

	Calibration		**Validation**			**Variables**
	Ranking (AICc)	R^2	R^2	RMSE (m)	RMSE_rel (%)	
$SI_{ex\text{-}post}$	1°	0.99	0.97	0.36	1	MMAX; TDIFF; Cab; LAI; Sand_10; Rad; Slope
	2°	0.98	0.95	0.45	1.29	MMAX; TDIFF; Cab; LAI; Sand_35; Delta_N_10
	3°	0.97	0.88	0.63	1.81	MMAX; TDIFF; Cab; LAI; Sand_35
	4°	0.96	0.89	0.67	1.93	MMAX; TDIFF; Sand_35; Delta_N_10; Age;
	5°	0.98	0.93	0.52	1.5	MMAX; TDIFF; Delta_N_10; Age; CN_35; WUEi

SI ex-ante	1°	0.73	0.58	1.29	3.7	CN_35; MMAX; MTWM
	2°	0.80	0.63	1.22	3.5	CN_35; MMAX; MTWM; Slope
	3°	0.77	0.52	1.41	4.1	CN_35; MMAX; MTWM; Delta_N_35
	4°	0.76	0.44	1.65	4.8	CN_35; MMAX; MTWM; Clay_35
	5°	0.76	0.55	1.41	4.1	CN_35; MMAX; MTWM; Altitude
SI simplified	1°	0.93	0.74	1.01	2.9	LAI; REIP; SUMP; Sum_surplus; Altitude; Rad
	2°	0.75	0.49	1.44	4.1	LAI; REIP; SUMP; Sum_surplus;
	3°	0.84	0.63	1.22	3.5	LAI; Cab; MTWM; Sum_deficit; Rad
	4°	0.62	0.44	1.49	4.3	LAI; Cab; MTWM;
	5°	0.84	0.57	1.35	3.9	LAI; Cab; MTWM; Sum_deficit; MMAX

Note: *Ranked by AICc; calibration R-squared (R^2) with bootstrap, validation R-squared (R^2) with LOOCV, root mean squared error (RMSE), relative root mean square error (RMSE_rel), variables included in the model (Variables).*

$$SI_{ex-ante} = 16.07 + (3.12\ MMAX) - (3.86\ MTWM) + (2.06\ CN\_35) - (3.41\ Slope)$$

Eq. 3 - Best Site Index model to predict the fertility ex-ante plantation.

The simplified models for SI were divided in two main groups of variables and only the LAI is highlighted in all the models. The superior results of best model were probably due to the highest number of variables, however the AICc ranking agreed with the R^2 ranking (Table 4).

$$SI_{simplified} = -1316 + (1.99\ REIP) - (12\ LAI) + (0.08\ Rad) - (0.71\ SUMP) + \\ + (0.04\ Sum\_surplus) - (0.009\ Altitude)$$

Eq. 4 - Best simplified Site Index model to explain fertility without field survey.

All the best models did not shown trends in the residuals and their frequency distributions were quite normal. The analysis of variance for the best models revealed that Rad, Altitude and REIP were not significant (p-value > 0.05) for the models, also the MMAX and Slope were not significant but only for the $SI_{ex\text{-}ante}$ model. Nevertheless, the other variables were all significant (p-value < 0.05).

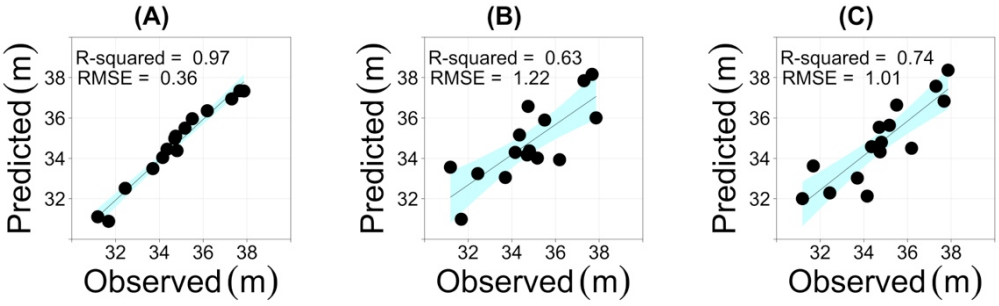

Figure 3 - Goodness of fit for the best Site Index models:

(A) SI $_{ex\text{-}post}$; (B) SI $_{ex\text{-}ante}$; (C) SI $_{simplified}$.

4.2 Net current annual increment

Since the small variability in trees age (eight years), the CAI_net has been proposed as fertility index ad fixed age.

The same protocol used for Site Index models was adopted for net current annual increment (CAI_net) and the results from the three models type were similar: the best results were for ex-post modeling, the worst were for ex-ante and the simplified reached mid-way results.

The $CAI_{ex\text{-}ante}$ and $CAI_{ex\text{-}post}$ models were agreed with the importance of Altitude variable since it was chosen always by the AICc selection, but the $CAI_{simplified}$ models did not corroborate this importance (Table 5)

The results and the variables selection for $CAI_{ex\text{-}post}$ models were very similar, in fact, the models were different from each other only for one o two variables. The Altitude, Sand_10, Sand_35, Delta_N_35, Rad were selected for all the models.

Table 5 - CAI net models summary.

	Calibration		**Validation**			**Variables**
	Ranking (AICc)	R^2	R^2	RMSE ($m^3/ha^{-1}/yr^{-1}$)	RMSE_rel (%)	
CAI ex-post	1°	0.99	0.98	0.96	6.1	Altitude; Sand_10; Sand_35; Delta_N_35; Rad; MTCI; FAPAR
	2°	0.98	0.96	1.37	8.6	Altitude; Sand_10; Sand_35; Delta_N_35; Rad; Cab
	3°	0.99	0.98	0.95	6	Altitude; Sand_10; Sand_35; Delta_N_35; Rad; Cab; REIP
	4°	0.99	0.96	1.22	7.7	Altitude; Sand_10; Sand_35; Delta_N_35; Rad; Cab; CN_35
	5°	0.99	0.97	1.12	7.1	Altitude; Sand_10; Sand_35; Delta_N_35; Rad; LAI; CN_35
CAI ex-ante	1°	0.64	0.43	5.97	37.8	Altitude; MMAX
	2°	0.53	0.30	6.63	42	Altitude
	3°	0.61	0.35	6.19	39.2	Altitude; Slope
	4°	0.71	0.50	5.15	32.6	Altitude; Slope; Sum_deficit
	5°	0.60	0.34	6.29	39.8	Altitude; Sand_10
CAI simplified	1°	0.63	0.53	4.42	27.9	LAI
	2°	0.70	0.56	4.29	27.1	LAI; Rad
	3°	0.68	0.53	4.46	28.2	LAI; FAPAR
	4°	0.68	0.50	5.15	32.6	LAI; Altitude
	5°	0.67	0.49	4.64	29.4	LAI; REIP

Note: *Calibration ranking during the selection of variables by AICc, R-squared (R^2) in calibration, R-squared (R^2) in validation, root mean squared error (RMSE), relative root mean square error (RMSE_rel), variables included in the model (Variables).*

$$\mathrm{CAI}_{ex-post} = -129 + (0.03\ \mathrm{Altitude}) - (2\ \mathrm{Sand\_10}) + (2.04\ \mathrm{Sand\_35}) - (2.88\ \mathrm{Delta\_N\_35}) - \\ -(0.25\ \mathrm{Rad}) + (4.88\ \mathrm{MTCI}) + (2.1\ \mathrm{FAPAR})$$

Eq. 5 - Best model to explain the CAI in Douglas fir plantation.

The ranking by AICc in $CAI_{ex\text{-}ante}$ models wasn't corroborate by R^2 results, the best model was the fourth, it was probably due to the highest number of variables in that model.

$$CAI_{ex-ante} = 8.49 + (0.03\ \text{Altitude}) - (0.14\ \text{Sum\_deficit}) - (13.86\ \text{Slope})$$

Eq. 6 - Best model to predict the CAI net

As for $CAI_{ex\text{-}ante}$ models, the $CAI_{simplified}$ models were able to explain only half of the total variance (Table 5). These results were due to the lower numbers of variables used in the models. Besides that, the diagnostic model ($CAI_{simplified}$) with only two variables overcame the prognostic one ($CAI_{ex\text{-}ante}$) because the CAI is much more related to LAI than Altitude.

$$CAI_{simplified} = -62.57 + (38.39\ \text{LAI}) - (0.19\ \text{Rad})$$

Eq. 7 - Best diagnostic CAI model with simplified method.

The analisis of variance (ANOVA) for the CAI best models shown a lack of significance only for Rad and Sum_deficit, p-value lower than 5%. Furthermore, any plot with fitted values against residuals did not shown particular pattern.

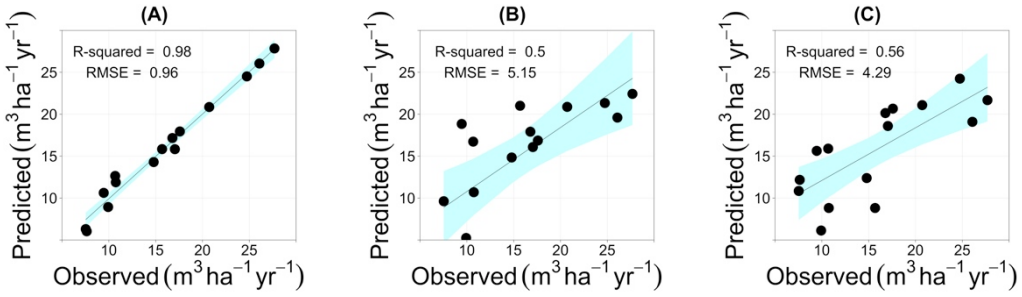

Figure 4 - Goodness of fit for the best CAI models:

(A) CAI $_{ex\text{-}post}$; (B) CAI $_{ex\text{-}ante}$; (C) CAI $_{simplified}$.

5 Discussion

Site index has always been the most used parameter to estimate the site fertility with the aim of evaluate the forest productivity (Maetzke and Nocentini, 1994). However, this assumption is based on the well know relation between high and growth, but it is possible to study directly the relation between site parameters and growth (current annual increment).

Therefore, instead of trying to estimate only the Site Index, we have studied the possibility to suggest volume current annual increment at fixed age as fertility index.

The outstanding results obtained are remarkable compared to other empirical models developed. A great result was reached thru MLR by Klinka e Carter (1990) with 84% of explained variance in calibration; afterward a lots of authors (Kimsey et al., 2008; Curt et al., 2001; Curt, 1999) have tried to achieve better results changing variables and model technics. Nevertheless, they didn't exceed the 42% of explained variance. Only an Italian study was able to overcame the average and explain 58% of variance (Corona et al., 1998). Furthermore, a recent study (Littke et al., 2016) was able to explain the 89% of site index variation during calibration and 66% on validation, but using boosted regression trees models.

Before going any further, it is necessary to highlights the principal limits of this study; these great results achieved were obtained with data from 15 site located in three valleys adjacent each other, hence these data cannot represent all the environmental variance of Italy, but they can be a good thrust to try of apply this method on bigger scale.

That said, the $SI_{ex\text{-}post}$ model achieved the 97% of explained variance, therefore it is a very good diagnostic model to predict SI at 50 years in a young douglas-fir plantation with only 0.36 m error. On the other hand, the prognostic model ($SI_{ex\text{-}ante}$) wasn't able to explain the same amount of variance, but this approach allows the users to estimate the land suitability for new plantations. Therefore, it is necessary for increasing the douglas fir plantation extensions.

At last, the $SI_{simplified}$ method is designed for users which need to accomplish these predictions with less efforts.

Moreover, about CAI models, the results were similar to those gained for SI, but the values obtained are directly the volume growth instead of fertility index.

5.1 Statistical approach

The application of multiple linear regression is simplistic for representing the eco-physiological relationship between growth and environment because most ecological variables shows a typical non-linear course (Aertsen et al., 2010) and the effect on growth is more complex than a multiple linear regression. However, this study wasn't focused only on eco-physiological explanation of growth rather on develop useful and user-friendly models.

Due to these reasons, the statistical approach was designed with the validation step. Similar studies, even with different model technics, bases their results only on calibration. These models are interesting on eco-physiological explanation, but on the other hand, they are not really tested to make prediction.

According on this difference between validation and calibration, every paper should highlight which method was used for the analysis, because often it isn't very clear if the results are from validation or calibration method.

5.2 Factors affecting fertility

The multiple linear regression was chosen even for its easy interpretable results, therefore every selected variable in the model has a straightforward relationship with the Site index and CAI, each one with a positive or negative effect.

Lots of climate variables computed by Rehfeldt et al. (2014) such as TDIFF, MTWM, MMAX were included in the models, these inclusions corroborate his thesis; i.e. the climate index are significantly related to the Douglas-fir growth range.

The positive effect of Sand_10 and Sand_35 showed the importance of the soil drainage for Douglas-fir, highlighted by Corona et al. (1998) in Italy and Tyler et al. (1996) in Scotland. About the positive effect of Sand_10, it is necessary to indicate an incongruent result in the $CAI_{ex\text{-}post}$ model.

The solar radiation (Rad) has different effect for CAI and SI models, but in both cases the ANOVA highlighted a lack of significance.

The geomorphological variables such as slope and altitude were probably incorporated in the models as surrogate variables for climate and soil condition (Tyler et al., 1996), moreover the importance of altitude on productivity study has been demonstrated repeatedly (Tyler et al., 1996; Worrell, 1987).

6 Conclusion

The potential growth of Douglas-fir in Italy is very high and the indigenous conifer cannot reach the same productivity (Corona et al., 1998). Looking around in the near European state, the Douglas-fir plantation are much more widely spreads (Curt et al., 2001) than Italy, thus it is reasonable to think at Douglas-fir plantation area expansion.

Nowadays some politics and governments drive in a different direction and try to limit the extension of the Douglas-fir because it is considered as not indigenous species. Today, after almost a century of Douglas-fir presence in Italy and lots of different studies, no serious disease has been observed (Corona et al., 1998; Ciancio et al., 1981) and it hasn't an invasive attitude. Therefore, the politics could be changing to stimulate the plantation and increase the wood production with a high productive species such as the Douglas-fir.

This study has performed good results in order to estimate the land suitability for the Douglas-fir plantation in Italy. These tools are crucial to allow good territorial planning and guide clever investments.

7 Bibliography

Aertsen, W., Kint, V., van Orshoven, J., Özkan, K., Muys, B., 2010. Comparison and ranking of different modelling techniques for prediction of site index in Mediterranean mountain forests. Ecol. Modell. 221, 1119–1130. doi:10.1016/j.ecolmodel.2010.01.007

Amaro, A., Reed, D., Soares, P., 2015. Modelling forest system. CABI Publishing, Cambridge. doi:10.1017/CBO9781107415324.004

Antisari, L.V., Falsone, G., Carbone, S., Marinari, S., Vianello, G., 2015. Douglas-fir reforestation in North Apennine (Italy): Performance on soil carbon sequestration, nutrients stock and microbial activity. Appl. Soil Ecol. 86, 82–90. doi:10.1016/j.apsoil.2014.09.009

Bernetti, G., 1965. Tavola cormometrica locale a doppia entrata della Pseudotsuga douglasii cresciuta nei boschi di origine artificiale dell'Appennino e Preappennino Toscano (Firenze). Ric. Sper. di dendrometria e auxometria. Ist. Assest. For. dell'Università di Firenze IV.

Bueis, T., Bravo, F., Pando, V., Turrión, M., 2016. Relationship between environmental parameters and Pinus sylvestris L. site index in forest plantations in northern Spain acidic plateau. iForest - Biogeosciences For. 8, e1–e8. doi:10.3832/ifor1600-008

Calcagno, V., Mazancourt, C. De, 2010. glmulti : An R Package for Easy Automated Model Selection with (Generalized) Linear Models. J. Stat. Softw. 34, 1–29. doi:10.18637/jss.v034.i12

Chevan, A., Sutherland, M., 1991. Hierarchical Partitioning. Am. Stat. 45, 90–96.

Ciancio, O., Eccher, A., Gemignani, G., 1980. Eucalitti, pino insigne, douglasia ed altre specie a rapido accrescimento. Ital. Agric. 117, 190–214.

Ciancio, O., Mercurio, R., Nocentini, S., 1981. Le Specie Forestali Esotiche nella Selvicoltura Italiana. Ann. dell' Ist. Sper. per la Selvic. 12–13, 1–690.

Corona, P., Scotti, R., Tarchiani, N., 1998. Relationship between environmental factors and site index in Douglas-fir plantations in central Italy. For. Ecol. Manage. 110, 195–207. doi:10.1016/S0378-

1127(98)00281-3

Curt, T., 1999. Predicting yield of Norway spruce and Douglas-fir using a morphopedological approach in the granitic landscapes of French Massif Central. Can. J. Soil Sci. 79, 491–500.

Curt, T., Bouchaud, M., Agrech, G., 2001. Predicting site index of Douglas-Fir plantations from ecological variables in the Massif Central area of France. For. Ecol. Manage. 149, 61–74. doi:10.1016/S0378-1127(00)00545-4

Curtis, R.O., 1967. Height-Diameter and Height-Diameter-Age Equations For Second-Growth Douglas-Fir. For. Sci. 13, 365–375.

Dash, J., Curran, P.J., 2004. MTCI: The meris terrestrial chlorophyll index. Eur. Sp. Agency, (Special Publ. ESA SP 151–161. doi:10.1080/0143116042000274015

Dlugokencky, E.J., Lang, P.M., Mund, J.W., Crotwell, A.M., Crotwell, M.J., Thoning, K.W., 2016. Atmospheric Carbon Dioxide Dry Air Mole Fractions from the NOAA ESRL Carbon Cycle Cooperative Global Air Sampling Network, 1968-2015. Version: 30/08/2016. ftp://aftp.cmdl.noaa.gov/data/trace_gases/co2/flask/surface/.

Ehleringer, J.R., Bowling, D.R., Flanagan, L.B., Fessenden, J., Helliker, B., Martinelli, L.A., Ometto, J.P., 2002. Stable Isotopes and Carbon Cycle Processes in Forests and Grasslands. Plant Biol. 4, 181–189.

Farquhar, G.D., Ehleringer, J.R.R., Hubick, K.T.T., 1989. Carbon isotope discrimination and photosynthesis. Annu. Rev. Plant Physiol. Plant Mol. Biol. 40, 503–537.

Farquhar, G.D., O'Leary, M.H., Berry, J.H., 1982. On the relationship between carbon isotope discrimination and intercellular carbon dioxide concentration in leaves. Aus.J.Plant Physiol. 121–137.

Gower, S.T., Kucharik, C.J., Norman, J.M., 1999. Direct and Indirect Estimation of Leaf Area Index, fAPAR, and Net Primary Production of Terrestrial Ecosystems. Remote Sens. Environ. 70, 29–51. doi:10.1016/S0034-4257(99)00056-5

Huld, T., Müller, R., Gambardella, A., 2012. A new solar radiation database for estimating PV performance in Europe and Africa. Sol. Energy 86, 1803–1815. doi:10.1016/j.solener.2012.03.006

Kahmen, A., Wanek, W., Buchmann, N., 2008. Foliar δ15N values characterize soil N cycling and reflect nitrate or ammonium preference of plants along a temperate grassland gradient. Oecologia 156, 861–870. doi:10.1007/s00442-008-1028-8

Kettler, T.A., Doran, J.W., Gilbert, T.L., 2001. Simplified method for soil particle-size determination to accompany soil-quality analyses. Soil Sci. Soc. Am. J. 65, 849–852.

Kimsey, M.J., Moore, J., McDaniel, P., 2008. A geographically weighted regression analysis of Douglas-fir site index in north central Idaho. For. Sci. 54, 356–366.

Klinka, K., Carter, R.E., 1990. Relationships between site index and synoptic environmental factors in immature coastal Douglas-fir stands. For. Sci. 36, 815–830.

Lavender, D.P., Hermann, R.K., 2014. Douglas-fir: The Genus Pseudotsuga. Oregon State University, Corvallis, OR.

Leonardi, S., Gentilesca, T., Guerrieri, R., Ripullone, F., Magnani, F., Mencuccini, M., Noije, T. V., Borghetti, M., 2012. Assessing the effects of nitrogen deposition and climate on carbon isotope discrimination and intrinsic water-use efficiency of angiosperm and conifer trees under rising CO 2 conditions. Glob. Chang. Biol. 18, 2925–2944. doi:10.1111/j.1365-2486.2012.02757.x

Littke, K.M., Harrison, R.B., Zabowski, D., 2016. Determining the Effects of Biogeoclimatic Properties on Different Site Index Systems of Douglas-fir in the Coastal Pacific Northwest. For. Sci. 62, 503–512.

Maetzke, F., Nocentini, S., 1994. L'accrescimento in altezza dominante e la stima della fertilità in Douglasia.

McCabe, G.J., Markstrom, S.L., 2007. A Monthly Water-Balance Model Driven By a Graphical User Interface, USGS Open-File Report 2007-1088.

Müller-Wilm, U., 2017. S2 MPC Sen2Cor Configuration and User Manual. doi:Ref. S2-PDGS-MPC-L2A-SUM-V2.4

O'Leary, M.H., 1993. Biochemical basis of carbon isotope fractionation, in: Stable Isotopes and Plant Carbon-Water Relations. Academic press, San Diego.

R_Core_team, 2016. R: A Language and Environment for Statistical Computing. R Foundation for Statistical Computing, Vienna, Austria. https://www.r-project.org/.

Rehfeldt, G.E., Jaquish, B.C., López-Upton, J., Sáenz-Romero, C., St Clair, J.B., Leites, L.P., Joyce, D.G., 2014. Comparative genetic responses to climate for the varieties of Pinus ponderosa and Pseudotsuga menziesii: Realized climate niches. For. Ecol. Manage. 324, 126–137. doi:10.1016/j.foreco.2014.02.035

Šúri, M., Huld, T.A., Dunlop, E.D., Ossenbrink, H.A., 2007. Potential of solar electricity generation in the European Union member states and candidate countries. Sol. Energy 81, 1295–1305. doi:10.1016/j.solener.2006.12.007

Templer, P.H., Arthur, M. a., Lovett, G.M., Weathers, K.C., 2007. Plant and soil natural abundance δ15N: Indicators of relative rates of nitrogen cycling in temperate forest ecosystems. Oecologia 153, 399–406. doi:10.1007/s00442-007-0746-7

Thornthwaite, C.W., Mather, J.R., 1957. Instructions and tables for computing potential evapotranspiration and the water balances, Climatology. Drexel Istitute of Technology, Centerton, New Jersey.

Tyler, A.L., Macmillan, D.C., Dutch, J., 1996. Models to predict the general yield class of Douglas fir, Japanese larch and Scots pine on better quality land in Scotland. Forestry 69, 13–24. doi:10.1093/forestry/69.1.13

Weiss, M., Baret, F., 2016. Sentinel2 ToolBox Level2 Products S2ToolBox Level 2 products: LAI, FAPAR, FCOVER Version 1.1.

White, J.W.C., Vaughn, B.H., Michel, S.E., 2015. Stable Isotopic Composition of Atmospheric Carbon

Dioxide (13C and 18O) from the NOAA ESRL Carbon Cycle Cooperative Global Air Sampling Network, 1990-2014. University of Colorado, Institute of Arctic and Alpine Research (INSTAAR). Version: 26/10/2015. ftp://aftp.cmdl.noaa.gov/data/trace_gases/co2c13/flask/.

Wilson, D.S., Maouire, D. a., 2009. Environmental basis of soil-site productivity relationships in ponderosa pine. Ecol. Monogr. 79, 595–617. doi:10.1890/08-0586.1

Worrell, R., 1987. Geographical variation in Sitka spruce productivity and its dependence on environmental factors. Edinburgh University.

Xiao, Z., Liang, S., Sun, R., 2018. Evaluation of three long time series for global fraction of absorbed photosynthetically active radiation (FAPAR) products. IEEE Trans. Geosci. Remote Sens. 56, 5509–5524. doi:10.1109/TGRS.2018.2818929

Zuur, A.F., Ieno, E.N., Smith, G.M., 2007. Statistics for Biology and Health, Tetrahedron Org. Chem. Ser. Springer, New York, NY. doi:10.1016/S1460-1567(08)10011-3

Chapter II – Evaluation of Sentinel-2 time series change detection for forest harvesting of variable intensity in temperate forests

1 Abstract

Robust data for forest harvesting in Italian forest are missing (Cesaro et al., 2019; Mori, 2019). These data are crucial for a correct control and management on a regional and national level for a natural resource like forests. The remote sensing data archive and access are growing now more than ever (Drusch et al., 2012; Wulder et al., 2012), they are creating an immense quantity of data with continuous updating. This remote sensing characteristics made it an affordable and reliable solution for a precise forest monitoring. Since many studies have already established different solutions for forest change detection (Reiche et al., 2018a; Hirschmugl et al., 2017b; Ryan et al., 2012; Asner et al., 2009), this study was focused on the application to Italian forest of one promising solution (Reiche et al., 2015a), developed on tropical forest. A practical tool for an easy application on a large scale was the goal. Keeping this in mind, cloud and seasonal problems were partially avoided for creating the NDVI and NBR time series from Sentinel-2 images.

The accuracy assessment based on error matrixes has returned comprehensive values of User, Producer and Overall Accuracy (UA, PA, OA) for control the algorithm results on spatial and temporal accuracy. Different harvesting techniques were considered and used to verify the detection capability with a different impact on the crown cover.

The best results were achieved using single NBR time series. it was able to reach PA and UA for spatial accuracy equal to 92 and 83 respectively. Furthermore, the detection was very good for all harvesting techniques assessed (PA values: clear-cut 99, coppice 95, thinning 94), the worst one was for conversion (PA 84).

2 Introduction

Change detection algorithm development for tropical forest are driven mainly by the need of quickly identify and quantify deforestation over large areas (Reiche et al., 2018a; Hirschmugl et al., 2017b; Ryan et al., 2012; Asner et al., 2009). Nevertheless, the importance of sustainable forest management is rapidly increasing in Europe and in the European Commission it's raising awareness (2013), therefore a reliable method for mapping and identify forest degradation and disturbance is fundamental. According to Intergovernmental Panel on Climate Change (IPCC) carbon report, forest degradation is clearly attributed to a *"direct human-induced activity that leads to a long-term reduction in forest carbon stocks".* Instead, the forest disturbance is commonly used to describe mainly natural effects on the forest biomass or crown cover, such as forest fire, drought stress, storm damage, insect infestation and may include short-term impact harvesting (Hirschmugl et al., 2017b).

Since the opening archive of Landsat data in 2008 (Wulder et al., 2012) many other space agencies followed the data policy from United States Geological Survey (USGS), for instance the European Space Agency (ESA) with the Sentinel-2 mission (Drusch et al., 2012). These datasets are growing now more than ever before and with such data volume in high spatial and temporal resolution, using time series analysis allow to carefully monitor changes in a national (Potapov et al., 2012) and global level (Hansen et al., 2013). However, forest types, seasonal effects as well as degradation drivers are geographic location related. Consequently, it's difficult to provide a reliable method with a very high detailed products able to satisfy managers and politics in a multilevel system (local, regional, national and global level). In this context the recently lunched Sentinel-2A and Sentinel-2B (in June 2015 and March 2017, respectively) are a feasible answer for a multilevel forest monitoring due to their high spatial resolution and sort revisit time.

2.1 Optical sensors problems

Anyhow all optical observations are facing some constrains which effect a time series analysis. First of all, the major problems for optical sensor in remote sensing are clouds and cloud shadow (Hirschmugl et al., 2017a; Zhu and Woodcock, 2014; Huang et al., 2010; Asner, 2001). The cloud problem is especially evident in change detection analysis because cloud contamination may be mapped as false changes (Huang et al., 2010). There are many methods for detect and mask cloud and cloud shadow (Zhu and Woodcock, 2012; Huang et al., 2010; Irish et al., 2006) but nowadays researchers are usually still avoiding the problem using cloud-free images (Tang et al., 2019; Grecchi

et al., 2017; White et al., 2017), although studying new procedure to improve cloud masking (Baetens et al., 2019).

For Sentinel-2, the European Space Agency (ESA) processor for converting images from Level-1C (Top Of Atmosphere) to Level-2A (Bottom Of Atmosphere) it's called Sen2Cor (Main-Knorn et al., 2017). During the atmospheric correction procedure, it generates a pixel classification map (cloud, cloud shadows, vegetation, soils/deserts, water, snow, etc.). This classified scene can be used to mask cloud and cloud shadow (Ranghetti and Busetto, 2019), but the accuracy is not perfect especially for cloud shadow and for cloud borders. For this purpose, Ranghetti and Busetto implemented in their procedure the possibility to add a buffer and smooth the mask (Ranghetti and Busetto, 2019).

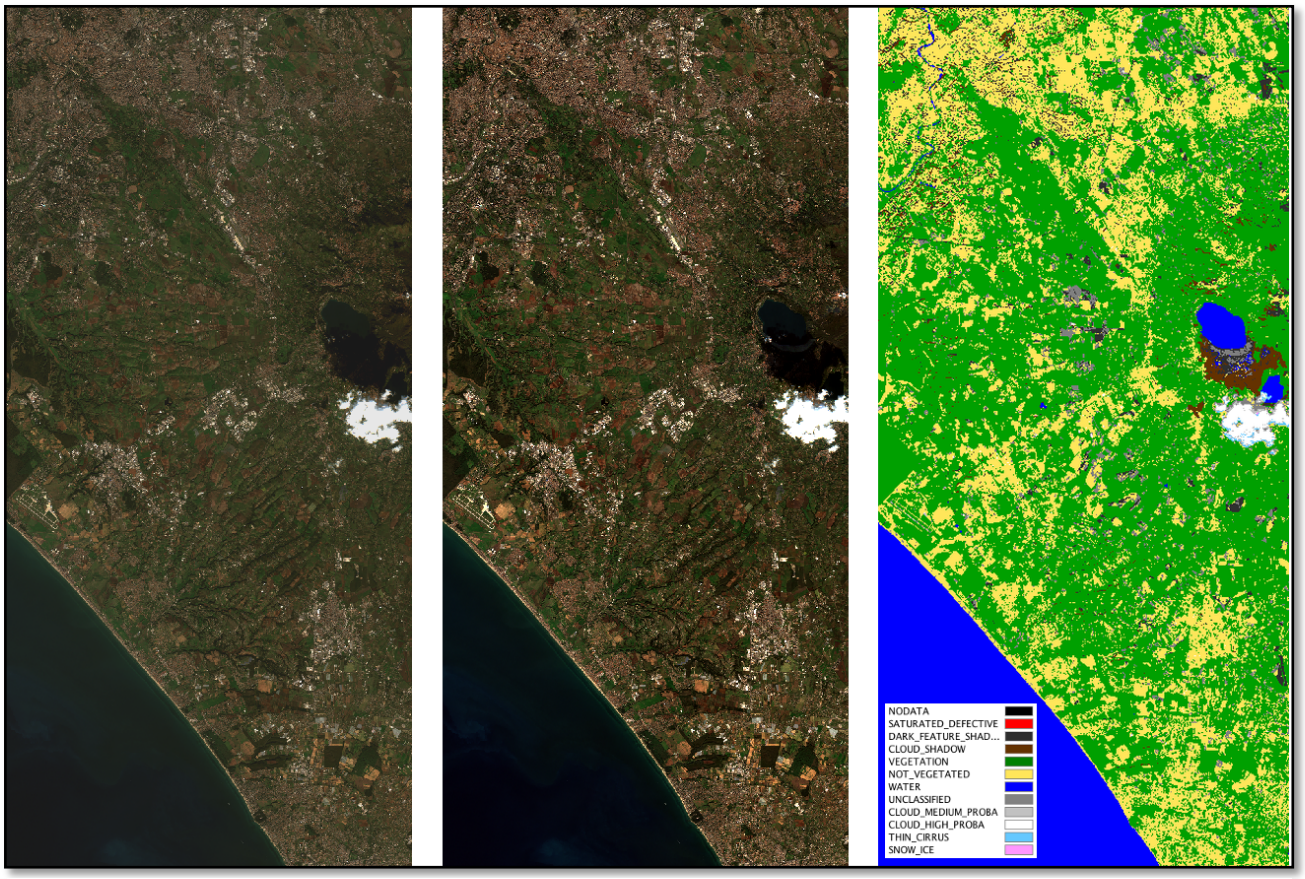

Figure 5 - SEN2COR processor generate Level-2A products with a scene classification for many classes including cloud and cloud shadow (ESA, 2019). from left to right: (1) Sentinel-2 Level-1C TOA reflectance input image, (2) the atmospherically corrected Level-2A BOA reflectance image, (3) the output scene classification of the Level-1C product.

Furthermore, the optical images are susceptible of seasonal or cyclic changes driven from annual temperature and rainfall interaction (Verbesselt et al., 2012), which impacts in plant phenology. This is particularly true in temperate zones, where four seasons are remarkably impacting in the plant crown appearance and characteristics. Using a time series approach, this effect is a real

concern and there are different techniques to address this issue (Reiche et al., 2015a, 2018a; Shimizu et al., 2017; Cai and Liu, 2015; Verbesselt et al., 2010), however these studies are made in tropical region with different forest and different seasonal cycle. Occasionally, a simple but effective workaround is used: excluding images in the useless period of the year (Shimizu et al., 2017); e.g. in winter trees are leaf-off and remote sensing signal is weaker than summer conditions for disturbance detection.

The clouds in temperate zones are present mainly during fall, winter and spring but in summer long cloud-free periods are common. Moreover, in summer the forest NDVI and NBR is much more different from the disturbance condition than in winter NDVI/NBR. In this regard, the study was focused on using a time series change detection approach excluding potential errors and complications. Therefore, only summer images (June, July, August) were used to compose the time series. In this way a simplified method developed for tropical forest was tested to perform change detection in temperate forests (Italian Apennine). This aim was addressed in order to potentially fill the lack of information present in the Italian forest sector about statistical data on forest harvesting.

This problem has a long history ending with the statistical data interruption in 2015 (Mori, 2019). As Mori (2019) wrote and Brosofske et al. (2014) reinforced, the potential for a statistical and inventory data produced from remote sensing techniques is more and more near to reality. Nowadays, the remote sensing data accessibility granted from space agencies all across the globe give a ready-to-use database of information never saw before. Although, a great number of change detection methodology has already been proofed and they show stunning results (Zhu, 2017). Since there aren't methodology tested in Italian forest, the aims of this study was to verify the application of a change detection method developed in tropical forest from Reiche et al. (2015a), which revealed a promising results. All the process was done bearing in mind the intention to upscaling the procedure to a nationwide level. Given all these circumstances, the procedure adopted was simplifier than the original method (Reiche et al., 2015a) in order to achieve the best result in the simplest way. Because of the future view to upscaling and deliver a practical tool for institutions and authorities interest in a frequent and precise forest harvest monitoring for statistical and management purpose.

3 Materials and methods

3.1 Study area

For this study, the area of interest was chosen based on the data availability and the possibility to find different logging techniques adopted in the period 2015-2018. In central north Apennines in the region of Emilia-Romagna, the authority designated to control and authorize the forest harvesting was able to share information about logging events during the period of interest, and so the province of Bologna was chosen.

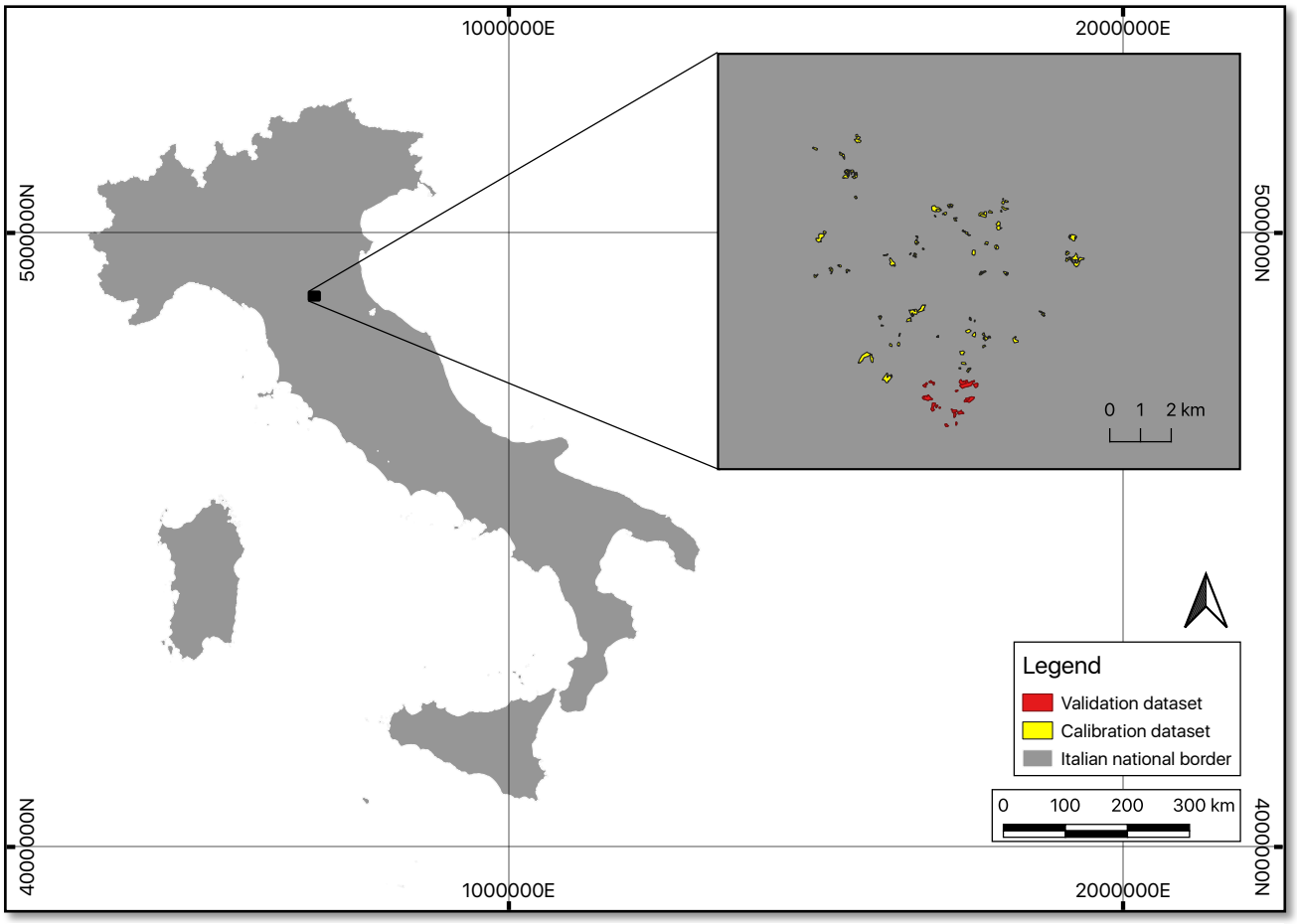

Figure 6 - Study area location, in the zoomed window are showed the dataset for calibration and validation.

In that area the forest is predominantly composed by broadleaf tree, but some planted conifer, such as *Pinus spp* and *Abies* are present as well. The forest management in coniferous stands is mainly based on thinning and clear-cut. On the other hand, the principal techniques in broadleaf stands are coppice with standards, conversion from coppice to high forest and thinning. All the previous mentioned practices are limited in intensity and extension by law, but the regulation give a per specie range of variation for the intensity.

The forest in this area has a long history of exploitation and harvesting, beside the period during the second world war two, the forest is growing faster than the harvesting rate. This condition assures the sustainability of the practice and clears any doubts about deforestation, in fact the forest extension is growing (Cesaro et al., 2019).

3.2 Bayesian multi-input time series approach

The time series change detection approach chosen is explained in detail by Reiche et. al. (2015a). This method is able to use multiple time series as input, no matter if they are coming from the same sensor o different one. It's based on non-forest conditional probability calculated on forest (F) and non-forest (NF) probability density functions. Each probability density function has to be defined for every time series used. The NF conditional probability at each time is determinate by iterative Bayesian updating, using previous, current and future observations to confirm or reject a forest disturbance. If the condition NF probability exceeds the defined threshold, a potential disturbance is flagged, in order to be confirmed the follow update has to be over the threshold as well, otherwise the mark will be removed.

The threshold value used is the same suggested by the authors (Reiche et al., 2015a) and correspond to 0.9. Furthermore, the probability density functions were estimated from a calibration dataset created from verified logging events in order to define parameters accurately calibrated on the study area.

3.3 Calibration and validation dataset

With the aim of assessing the potential of this change detection method in Italian forest, using a local database for calibration and validation is crucial. The calibration dataset extension is about 7200 ha, however the forested area is 4050 ha based on the regional forest map updated on 2014.

The forest probability density function was calculated over this 4050 ha excluding the known logging surface. As shown in Table 6, the harvested surface is much less than the undisturbed one, but this represent almost the total harvest in the period 2015-2018 classified by the logging techniques adopted. It was used this area to calibrate the parameters because the large variety of cut extension and techniques, but the database wasn't included all the logging events in the reference period (2015-2018). This is due to the lack of information in the Italian forest sector. The database was

created with the help of forest control authority (Unione dei comuni), a field survey and some photointerpretation from satellite very high-resolution images but even with all this effort was impossible to create a complete database as large as this with all the logging events.

As displayed in Figure 7, the validation dataset was a nearby area of calibration dataset without overlapping. This was necessary in order to properly verify the change detection results on an independent dataset. The area was much smaller than the calibration dataset and correspond to about 400 ha. Adopting a smaller area allow to clearly identify all the cuts executed in the period 2015-2018 and inventory it in order to have a complete reference dataset (see Figure 8).

Table 6 – Statistical summary for calibration database, the high number of coppice cut show the importance of this technique in the study area.

Harvesting type	*Number of areas*	*Average extension (ha)*	*Min extension (ha)*	*Max extension (ha)*	*Total extension (ha)*	*Pixel extension (S-2 grid)*
Coppice	101	0.7	0.09	3.22	71.35	7110
Clear cut	18	1.00	0.10	4.5	19.75	1974
Thinning	8	2.55	0.57	4.9	20.45	2032
Conversion	3	2.57	1.26	5.00	7.72	768
Tot summary	*130*	*0.92*	*0.09*	*5.00*	*119.3*	*11884*

The validation areas collected from institutions was checked by field survey in order to reach the best reliability. Since the area was limited, it was possible to verify every harvested areas using GPS and confirm the year of the events by expert looking at forest regrowth. The field survey was done in 2018 with the Holux funtrek 130 pro GPS, following indications from loggers and also searching by looking in the valley. It was chosen this area because it represents a common Apennines area and the harvesting intensity is standard. The predominant cutting techniques is coppice with

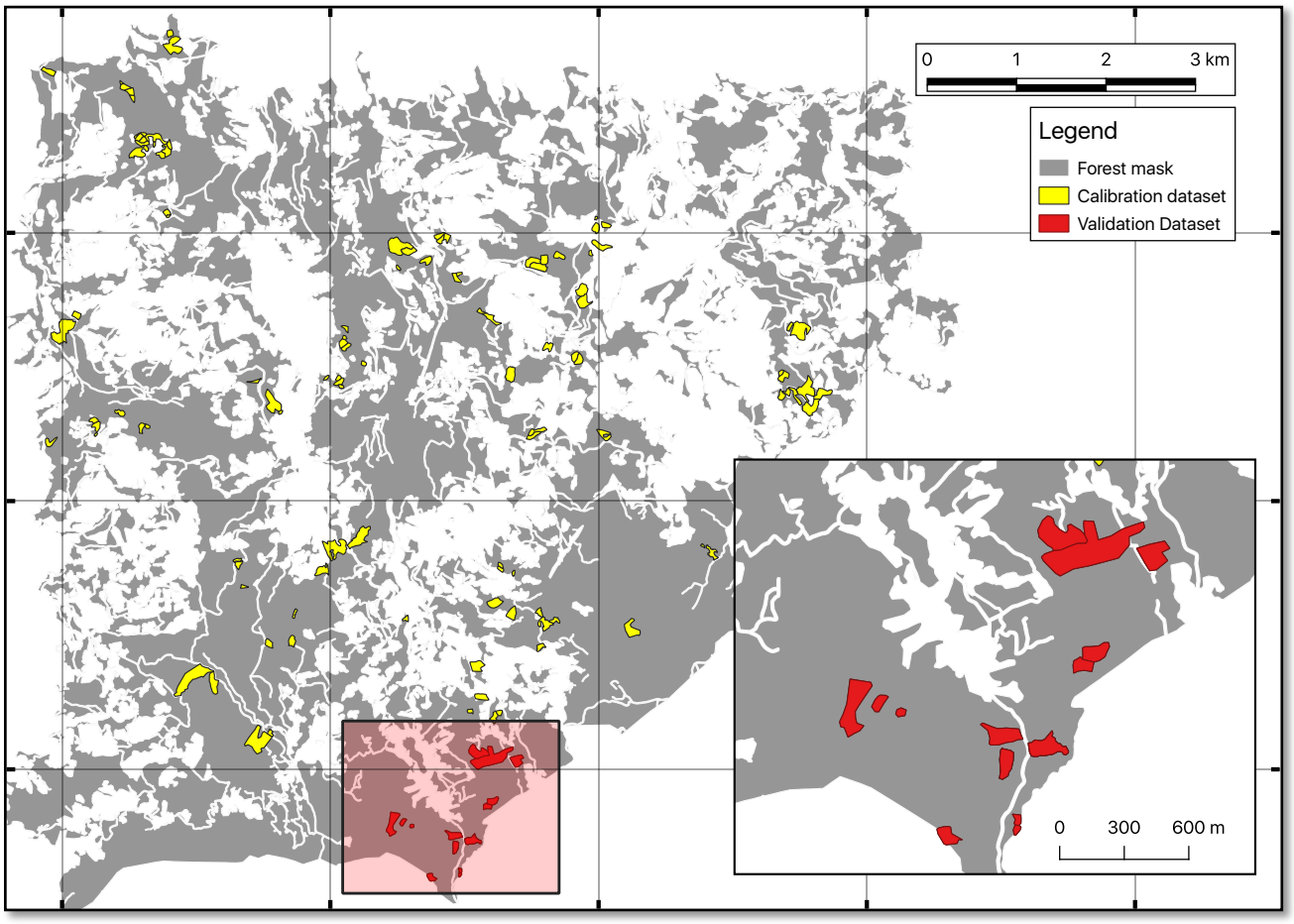

Figure 7 - Database of logging events from 2015 to 2018 for calibrate the probability density functions (yellow) and for validate and assessing (Red) the accuracy for the change detection method.

standards, although other are present, they are only occasionally and less frequent. These characteristics and the certainty of the forest and non-forest surface made this part of the dataset a good area for the validation process.

As shown in the Table 7, beside the coppice cuts, the other typologies were represented from a few events (see Figure 8 as well). The number correspond to the entire surface event, which always correspond to more than one hectare surface. This extension divided by the Sentinel-2 pixel grid (10m pixel) results in a large number of pixels. While the change detection is by pixel, this resolve the problem of the low number of clear-cut, thinning and conversion.

Table 7 -Statistical summary for validation database.

Harvesting Type	*Number of areas*	*Average extension (ha)*	*Min extension (ha)*	*Max extension (ha)*	*Total extension (ha)*	*Pixel extension (S-2 grid)*
Coppice	10	0.62	0.11	1.88	6.2	600
Clear cut	1	1.15	1.15	1.15	1.15	119
Thinning	1	2	2	2	2	201
Conversion	2	3.13	1.26	5.00	6.26	617
Tot summary	*14*	*1.12*	*0.11*	*5.00*	*15.62*	*1537*

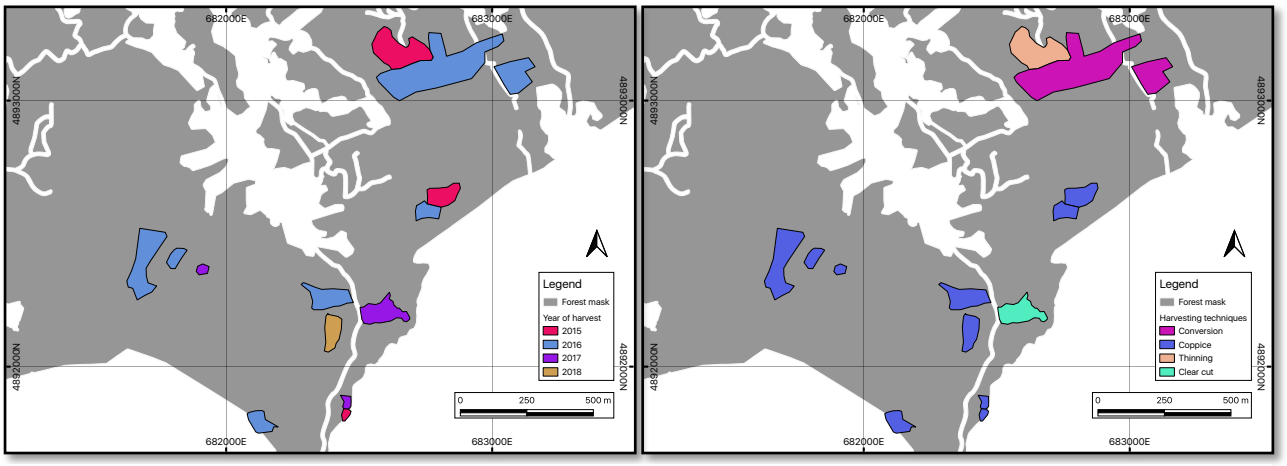

Figure 8 - Validation dataset classified by year (on the left) and harvesting techniques (on the right)

3.4 Sentinel-2 data and pre-process workflow

Sentinel-2 is a European Space Agency (ESA) mission with two satellites working in tandem. Each satellite carry a multispectral optic camera capable of capture 13 spectral bands images in high spatial resolution (varying by band) and high revisit frequency (5 days at the equator) (Sentinel-2 PDGS Project Team, 2011). Indeed, this high frequency revisit time is due to the couple work of the two satellite.

For the time series construction were used only summer (June, July, August) images from 2015 to 2018. A total of 39 images (see Figure 9) were selected due to the threshold of 20% of cloud cover. The dataset download was executed from the Copernicus Open Access Hub thru the API access.

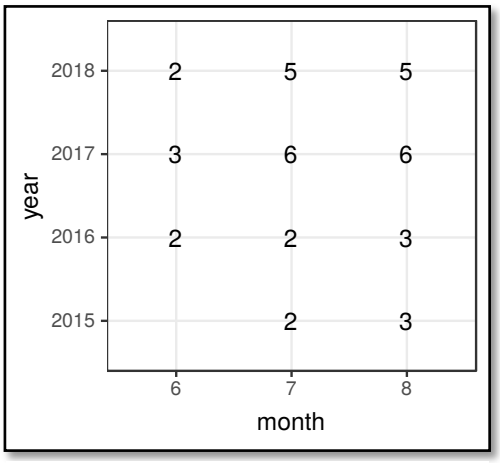

Figure 9 - Number of Sentinel-2 images per month with a total amount of 39 images.

Since the L2A images were not available for all the 2015-2018 period, only L1C level images were downloaded in order to apply the exact same pre-process workflow to all the images.

The well-known SEN2COR (Main-Knorn et al., 2017; Müller-Wilm, 2017) processor (atmospheric radiative transfer) was applied to the L1C images in order to obtain L2A images. L2A product level consist in Bottom of Atmosphere (BOA) corrected reflectance images, with terrain and cirrus correction as well.

All the pre-process workflow was completed using the Sen2r package (Ranghetti and Busetto, 2019) implemented in the R (R_Core_team, 2016) programming language. This package allows to use SEN2COR with other options, such as cloud masking and indices calculation. Indeed, it was used the cloud masking option with a 100m buffer and a value of 30 for the buffer smoothing. All the classified scenes (SCL) made from SEN2COR processor were applied for the cloud masking. This procedure was adopted despite losing pixels because in a time series change detection approach is better a lack of information instead of a wrong pixel value; it could drive to detection errors.

Therefore, in the same R package Normalized Burned Ratio (NBR)(Key and Benson, 2006) and Normalized Difference Vegetation Index (NDVI) were calculated because of their sensitivity to the forest disturbance (Shimizu et al., 2017; Grogan et al., 2015). Together the time series were used in order to obtain a better change detection, since the NDVI after disturbance is rapidly rising and tends to saturate easily, while the NBR is more strongly linked to forest structure (White et al.,

2017). Both indices are widely use in literature per forest fire and forest disturbance detection and estimation (Lima et al., 2019; White et al., 2017; Cohen et al., 2010; Vicente-Serrano et al., 2008; Wimberly and Reilly, 2006; Cocke A,B et al., 2005).

$$NBR = \frac{NIR - SWIR2}{NIR + SWIR2}$$

$$NDVI = \frac{NIR - RED}{NIR + RED}$$

Eq. 8 - Normalized Burned Ration equation (on top), Normalized Difference Vegetation Index equation (on bottom).

3.5 Calibration method

As previously mentioned in the paragraph 3.3, A set of ground truth areas were selected for the calibration process, namely, calculate the probability density function (pdf) for forest (F) and non-forest (NF) areas. For both NDVI and NBR time series the pdfs were calculated with the same method. The forest pdf was based on the real values distribution of pixels inside the forest mask but outside the disturbed areas (according with the calibration dataset).

On the other hand, non-forest pdf was calculated using pixels inside the disturbed areas but considering only the year after logging events (according with the calibration dataset), i.e. excluding images before the events and after one year. With the aim of highlight the real index value deriving from the harvest and avoid potential noise from regrowth. Therefore, the total number of pixels used were 7454 for non-forest and 93034 for forest pixels.

The needed parameters for the change detection procedure were mean and standard deviation for F and NF distribution, but instead of using mean it was used the median value to reduce the effect of outliers.

3.6 Results assessment

Assessing change detection is largely discussed in literature (Olofsson et al., 2014; Liu and Zhou, 2004; Macleod and Congalton, 1998; Congalton, 1991), the most common and interpretable method was chosen to assess the results. All the procedures were based on the error matrix, this

allow to calculate accuracy parameters such as the Producer Accuracy (PA) i.e. the complementary of commission error, User Accuracy (UA) i.e. the complementary of omission error and lastly the Overall Accuracy (OA). The kappa value was intentionally avoided due to the large number of problems related, a very good explanation on that was given from Olofsson et. al. (2014).

Thankfully to the information available in the validation dataset it was possible to deeply assess the results. The investigation aimed to verify spatial and temporal accuracy as well as the detection ability for different harvesting techniques. The validation dataset contained the polygon shape of the harvesting areas linked with information on the type and year of logging event.

Initially the temporal accuracy was verified using a rasterized version of the validation dataset applying years for pixels values. This raster and that one obtained from the change detection algorithm were compared in the error matrix adopting the years (2015 to 2018) as classes plus the not disturbed area (no cut).

Subsequently the spatial accuracy was assessed using simplified validation dataset, all the areas were converted in “cut” and “no-cut” raster, as well as the output generated from the change detection algorithm. Then the error matrix was calculated based on these two simple classes.

Lastly, in order to assess the detection ability for different harvest technique, the validation dataset was modified for each class. For every class (coppice, clear-cut, thinning and conversion) the reference raster and the predicted raster were subtracted with the unused classes, e.g. when the “coppice” class was assessed in the clear-cut, thinning and conversion areas pixels values were set to no-data.

3.7 Change detection algorithm application

The chosen change detection algorithm (Reiche et al., 2015a) works with a single time series in input, but it’s able to fuse two or more time series as well. Since the needed parameters were estimated for NBR and NDVI time series, the algorithm was applied three times: once for NBR and NDVI singularly and lastly the NBR and NDVI fusion was tried.

From the time when the first date in the time series was 04/07/2015 the parameter to indicate the starting point was set to 2015.6. Moreover, the last parameter needed was the threshold of deforestation probability at which flagged change is confirmed; according to Reiche et al. (2015a) it was used a value of 0.9.

Since the change detection algorithm is a computing intensive data process, all the images pre-processing and the actual change detection procedure were executed in the computing environment provided by European Space Agency thru the Research and User Support service (RUS).

4 Results

The results presented in this chapter were obtained after a calibration to Italian forests of the change detection procedure developed by Reiche et al. (2015a) in tropical forest.

During the calibration, the Forest and Non-Forest pixel distribution (see Figure 10) highlighted the F-NF separability at pixel level, and the similarity between NBR and NDVI as well. The Forest means were 0.66 and 0.87 with a standard deviation of 0.09 and 0.07 for NBR and NDVI respectively. On the other hand, the Non-Forest means were 0.32 (NBR) and 0.60 (NDVI) with a standard deviation of 0.13 for both NBR and NDVI.

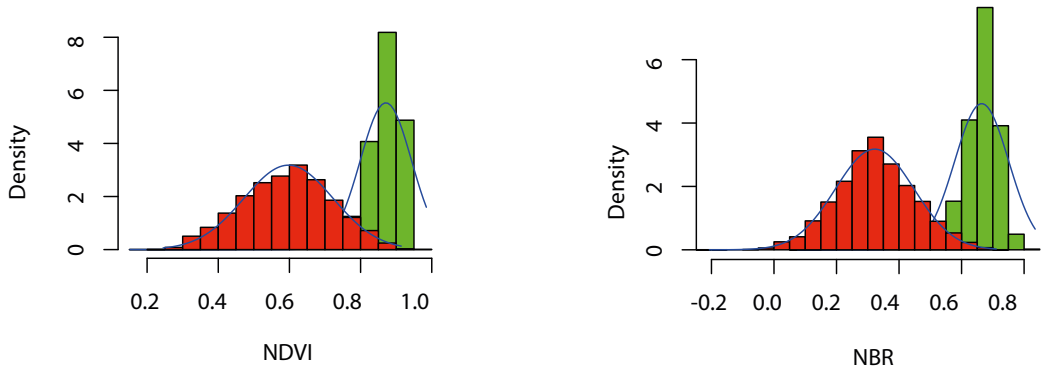

Figure 10 – NDVI and NBR histogram of frequency for non-forest (red) and forest (green) pixels.

As explained in the materials and methods (paragraph 3.6), after the change detection procedure, three error matrixes were made in order to assess different aspects such as spatial-temporal accuracy and forest harvesting techniques detectability.

The output map delivered from change detection procedure represented confirmed changes with a date value in Day Of Year (DOY). Then, the output raster was reclassified by years to match the reference classes (Figure 11 and Figure 12). Afterwards, the classes in the output map were used in the error matrix to compute the overall, user and producer accuracy (OA, UA, PA). With this type of assessment spatial and temporal accuracy was addressed together and this affect hardly the accuracy levels in the single class. So as to give a general description the mean UA and PA were calculated (Table 8), as well as the Overall accuracy: 95.9 for NBR, 96 for NDVI and 95.8 for the fusion of both NBR and NDVI time series. The class trends were quite similar between NBR and NDVI, the fusion of both indices didn't increase the results significantly, rather it reach usually an intermediate result between the results obtained with single time series (Table 8).

Table 8 - Change detection results for spatial and temporal accuracy assessment

	NBR		*NDVI*		*NBR and NDVI*	
	UA	PA	UA	PA	UA	PA
no cut	99.1	97.2	98.8	97.7	99.1	97.1
2015	45.1	99.6	57.2	99.6	47.2	99.6
2016	86.3	65.4	90.1	55.6	87.7	63.2
2017	27.9	93.2	25.7	91.8	25.4	94.5
2018	57.8	90.0	49.6	95.7	52.4	94.3
mean	63.2	89.1	64.3	88.1	62.4	89.7

With a view to practical application, the temporal component was excluded from the accuracy assessment converting all the pixel in only two classes: cut and no-cut. Only the spatial accuracy was assessed and in this case the result increased significantly compared to the previous assessment, especially for UA (Table 9). The overall accuracy reached little better results: 96.6 for NBR, 96.7 for NDVI and 96.5 for the fusion of both NBR and NDVI. As before, the time series fusion didn't increase the results.

Table 9 - Change detection results for simplified classes "cut" "no-cut"

	NBR		*NDVI*		*NBR and NDVI*	
	UA	PA	UA	PA	UA	PA
no cut	99.1	97.2	98.8	97.7	99.1	97.1
cut	65.8	86.1	68.9	80.5	65.3	85.7
mean	82.5	91.7	83.9	89.1	82.2	91.4

Results shown in Table 10 are little confusing, it's due to the method employed (explained in paragraph 3.6). The UA values were largely affected by the methodology as well as OA, which changed thru classes because the reference data was changed too.

A comprehensive looking to all the results highlighted some general trends. Between the three trial there wasn't a supreme one, but the fusion of two time series (NBR and NDVI) has never shown superior results rather an intermediate or even lower.

Table 10 - Chance detection results for different forest harvesting techniques

	NBR			*NDVI*			*NBR and NDVI*		
	UA	PA	OA	UA	PA	OA	UA	PA	OA
Clear cut	60.5	99.2	98.3	61.7	99.3	98.5	60.1	99.1	98.2
Coppice	74.4	95.2	97.6	76.1	93.0	97.9	74.0	95.3	97.5
Thinning	64.1	94.2	98.2	65.6	94.0	98.5	63.5	94.1	98.1
Conversion	74.2	83.6	97.6	74.0	79.1	97.6	73.1	82.9	97.5

5 Discussion

To better understand the results shown in Table 8, Table 9 and Table 10, looking at the Figure 11 and Figure 12 is very important because they give a real perception of the errors and the relative causes.

In Table 8 the UA and PA were changed drastically thru the classes. To explain this effect, looking at Figure 11 is crucial. It was clear that some cuts were done in multiple times, e.g. starting in one year and ending the follow or second year after. This problem affected the accuracy assessment in a negative way for both UA and PA, but this problem was actually related to a reference data issue. The change detection algorithm was able to identify very small (pixelwise) changes, way smaller than available reference data. Besides that, in 2015 and 2017 the UA was significantly lower than other years because of the major number of erroneous detected pixels were in 2015 and 2017 classes. On the contrary, the lower PA value in 2016 was due to the omission of the conversion cut executed in the northern-east area.

For a practical use, sometimes spatial accuracy is preferred than extreme temporal accuracy. Since the aim of this study wasn't test a near-real-time application, the second assessment focused on a spatial accuracy without temporal interference. It was also done to clarify the nature of errors. This revealed a great potential due to the high PA value (86 for harvest and 97 for not harvest areas), it's mean that only little parts of harvested areas were omitted. The omission error was primarily due to the conversion cut (Figure 11), which affect the crown cover only partially, similar to selective logging and hence it was more difficult to be detected from remote sensing optic images (Asner et al., 2005).

Looking at Figure 11, beside some margin errors due to images misregistration (Yan et al., 2018) and geolocation errors, the main commission errors, highlighted in the upper image (Figure 11) with circles, impacted negatively to the UA cut class (65.8 and 68.9 for NBR and NDVI respectively). Investigating further using Google Earth historical images, these areas were identified as old (before 2015) harvested areas, in fact the change detection algorithm identified these changes as soon as the time series started (2015).

Regarding the detection ability for harvest techniques, the different number of pixels per class in the reference area was responsible for some distortion in the results. In order to calculate the accuracy table, the output map was masked with the validation dataset excluding all the harvested areas beside the assessed one. The OA was changing by class and the UA was distorted because the

unused classes margin errors remained in the output map and became a commission error. This effect influenced especially the classes with a low number of pixels such as clear-cut and conversion. On the contrary, the PA was correctly assessed, the results were overwhelmed for the high level of accuracy reached: 99 for clear-cut, 95 for coppice, 94 for thinning and 84 for conversion. Moreover, the PA results were as expected: better with increasing crown cover disturbance, e.g. higher PA with clear-cut (complete crown cover removal) and lower PA for conversion (little effect on crown cover).

Furthermore, all results achieved with the fusion of NBR and NDVI agreed. No accuracy gain was reached, usually a midway or even lower results. This was probably due to the similarity of NBR and NDVI, which brought similar information. In fact, comparing Figure 11 with Figure 12, it was clear that PA was similar to the best results i.e. NBR time series, but the commission errors has been influenced from both NBR and NDVI lowering the UA.

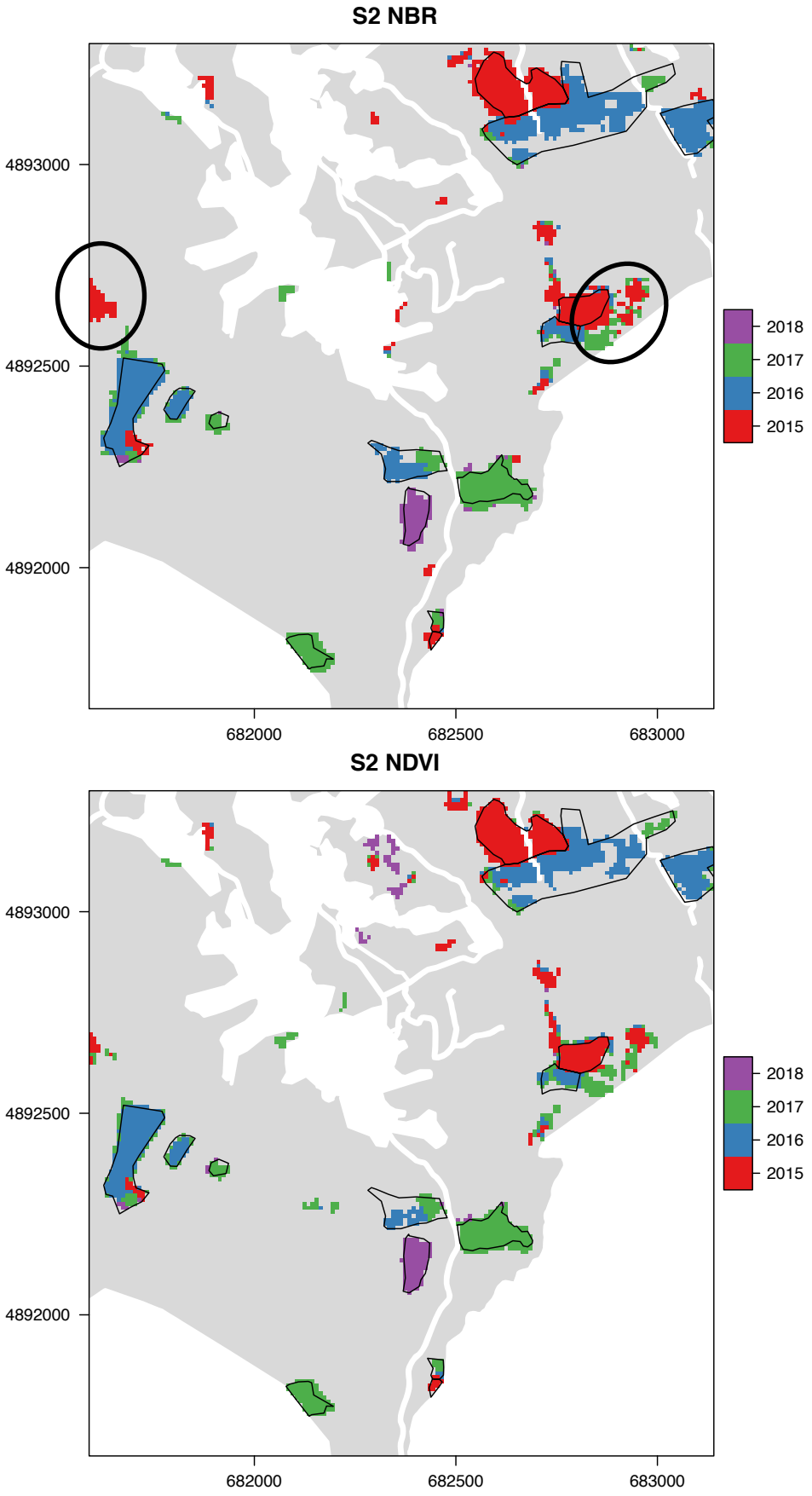

Figure 11 - NBR and NDVI change detection maps. In the upper image, two black circles indicate the main commission errors areas due to old harvest areas (before 2015).

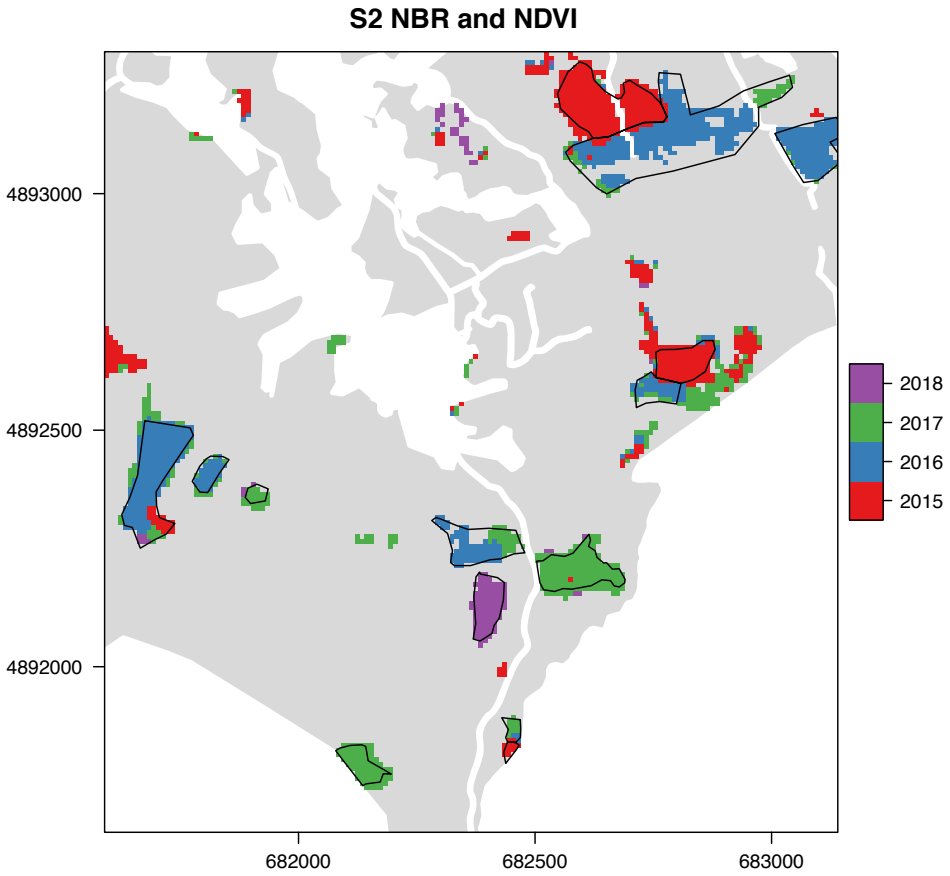

Figure 12 – Output map from NBR and NDVI time series fuse together

6 Conclusion

Forest change detection algorithm application to Italian and European forest is a procedure that it's raising attention (Mori, 2019; European_Commission, 2013). This study tried to find solutions to this in a rapid and easy way that it makes suitable for application in forest statistics, control and management. Using a single NBR time series was the best solutions and applying a fusion approach with NBR and NDVI didn't improved the results. A comprehensive spatial and temporal accuracy assessment was difficult due to the lack of ground-truth information, but positive results were achieved. Moreover, a deeper analysis based on Google Earth historical images and expert evaluation of harvesting practices revealed that algorithm had a better temporal resolution than validation dataset, it was capable of detect forest harvests executed on multiple years.

This simplified method is ready to be used for control, statistics and management on sub-regional level due to the computational effort needed. But upscaling is possible with adequate computational power and with a procedure optimization.

Future prospective could lead to the application of this change detection procedure with a whole year time series, using deseasonalize process with the aim of reaching an even better temporal accuracy (Reiche et al., 2018b, 2018a).

7 Bibliography

Asner, G.P., 2001. Cloud cover in Landsat observations of the Brazilian Amazon. Int. J. Remote Sens. 22, 3855–3862. doi:10.1080/01431160010006926

Asner, G.P., Knapp, D.E., Balaji, A., Páez-acosta, G., 2009. Automated mapping of tropical deforestation and forest degradation : CLASlite. J. Appl. Remote Sens. 3, 1–24. doi:10.1117/1.3223675

Asner, G.P., Knapp, D.E., Broadbent, E.N., Oliveira, P.J.C., Keller, M., Silva, J.N., 2005. Selective Logging in the Brazilian Amazon. Science (80-.). 310, 480–482. doi:10.1126/science.1118051

Baetens, L., Desjardins, C., Hagolle, O., 2019. Validation of copernicus Sentinel-2 cloud masks obtained from MAJA, Sen2Cor, and FMask processors using reference cloud masks generated with a supervised active learning procedure. Remote Sens. 11. doi:10.3390/rs11040433

Brosofske, K.D., Froese, R.E., Falkowski, M.J., Banskota, A., 2014. A Review of Methods for Mapping and Prediction of Inventory Attributes for Operational Forest Management. For. Sci. 60, 733–756. doi:10.5849/forsci.12-134

Cai, S., Liu, D., 2015. Detecting change dates from dense satellite time series using a sub-annual change detection algorithm. Remote Sens. 7, 8705–8727. doi:10.3390/rs70708705

Cesaro, L., Romano, R., Pompei, E., Piloni, S., Mori, P., Torreggiani, L., 2019. RaF Italia 2017-2018, Direzione generale delle foreste del Mipaaft. Arezzo.

Cocke A,B, A.E., Fulé, P.Z., Crouse, J.E., 2005. Comparison of burn severity assessments using Differenced Normalized Burn Ratio and ground data. Int. J. Wildl. Fire 14, 189–198. doi:10.1071/WF04010

Cohen, W.B., Yang, Z., Kennedy, R., 2010. Detecting trends in forest disturbance and recovery using yearly Landsat time series: 2. TimeSync — Tools for calibration and validation. doi:10.1016/j.rse.2010.07.010

Congalton, R.G., 1991. A review of assessing the accuracy of classifications of remotely sensed data. Remote Sens. Environ. 37, 35–46. doi:10.1016/0034-4257(91)90048-B

Drusch, M., Del Bello, U., Carlier, S., Colin, O., Fernandez, V., Gascon, F., Hoersch, B., Isola, C., Laberinti, P., Martimort, P., Meygret, A., Spoto, F., Sy, O., Marchese, F., Bargellini, P., 2012. Sentinel-2: ESA's Optical High-Resolution Mission for GMES Operational Services. Remote Sens. Environ. 120, 25–36. doi:10.1016/j.rse.2011.11.026

ESA, 2019. User guide - Sentinel2 MSI level2A [WWW Document]. URL https://sentinel.esa.int/web/sentinel/user-guides/sentinel-2-msi/processing-levels/level-2 (accessed 9.19.19).

European_Commission, 2013. A new EU Forest Strategy: for forests and the forest-based sector. Brussels.

Grecchi, R.C., Beuchle, R., Shimabukuro, Y.E., Aragão, L.E.O.C., Arai, E., Simonetti, D., Achard, F., 2017. An integrated remote sensing and GIS approach for monitoring areas affected by selective logging: A case study in northern Mato Grosso, Brazilian Amazon. Int J Appl Earth Obs Geoinf. 61, 70–80. doi:10.1016/j.jag.2017.05.001

Grogan, K., Pflugmacher, D., Hostert, P., Kennedy, R., Fensholt, R., 2015. Cross-border forest disturbance and the role of natural rubber in mainland Southeast Asia using annual Landsat time series. Remote Sens. Environ. 169, 438–453. doi:10.1016/j.rse.2015.03.001

Hansen, M.C., Potapov, P. V., Moore, R., Hancher, M., Turubanova, S.A., Tyukavina, A., Thau, D., Stehman, S. V., Goetz, S.J., Loveland, T.R., Kommareddy, A., Egorov, A., Chini, L., Justice, C.O., Townshend, J.R.G., 2013. High-Resolution Global Maps of 21st-Century Forest Cover Change. Science (80-.). 342, 850–853. doi:10.1126/science.1244693

Hirschmugl, M., Deutscher, J., Gutjahr, K., Sobe, C., Schardt, M., 2017a. Combined Use of SAR and Optical Time Series Data for Near Real-Time Forest Disturbance Mapping, in: 9th International Workshop on the Analysis of Multitemporal Remote Sensing Images. IEEE. doi:10.1109/Multi-Temp.2017.8035208

Hirschmugl, M., Gallaun, H., Dees, M., Datta, P., Deutscher, J., Koutsias, N., Schardt, M., 2017b. Methods for Mapping Forest Disturbance and Degradation from Optical Earth Observation Data: a Review. Curr. For. Reports 3, 32–45. doi:10.1007/s40725-017-0047-2

Huang, C., Thomas, N., Goward, S.N., Masek, J.G., Zhu, Z., Townshend, J.R.G., Vogelmann, J.E., 2010. Automated masking of cloud and cloud shadow for forest change analysis using Landsat images. Int. J. Remote Sens. 31, 5449–5464. doi:10.1080/01431160903369642

Irish, R., Barker, J., Goward, S., Arvidson, T., 2006. Characterization of the Landsat-7 ETM? Automated Cloud-Cover Assessment (ACCA) Algorithm. Photogramm. Eng. Remote Sens. 72, 1179–1188.

Key, C.H., Benson, N.C., 2006. Landscape Assessment (LA).

Lima, T.A., Beuchle, R., Langner, A., Grecchi, R.C., Griess, V.C., Achard, F., 2019. Comparing Sentinel-2 MSI and Landsat 8 OLI Imagery for Monitoring Selective Logging in the Brazilian Amazon. Remote Sens. 11, 961. doi:10.3390/rs11080961

Liu, H., Zhou, Q., 2004. Accuracy analysis of remote sensing change detection by rule-based rationality evaluation with post-classification comparison. Int. J. Remote Sens. 25, 1037–1050. doi:10.1080/0143116031000150004

Macleod, R.D., Congalton, R.G., 1998. A Quantitative Comparison of Change-Detection Algorithms for Monitoring Eelgrass from Remotely Sensed Data. Photogramm. Eng. Remote Sens. 64, 207–216.

Main-Knorn, M., Pflug, B., Louis, J., Debaecker, V., Müller-Wilm, U., Gascon, F., 2017. Sen2Cor for Sentinel-2. Proc. SPIE SPIEDigitalLibrary.org/conference-proceedings-of-spie. doi:10.1117/12.2278218

Mori, P., 2019. Statistiche forestali: Potenzialità e opportunità per ripartire da zero. Sherwood - For. ed alberi oggi 13–15. doi:ISSN 1590-7805

Müller-Wilm, U., 2017. S2 MPC Sen2Cor Configuration and User Manual. doi:Ref. S2-PDGS-MPC-

L2A-SUM-V2.4

Olofsson, P., Foody, G.M., Herold, M., Stehman, S. V., Woodcock, C.E., Wulder, M.A., 2014. Good practices for estimating area and assessing accuracy of land change. Remote Sens. Environ. 148, 42–57. doi:10.1016/J.RSE.2014.02.015

Potapov, P. V., Turubanova, S.A., Hansen, M.C., Adusei, B., Broich, M., Altstatt, A., Mane, L., Justice, C.O., 2012. Quantifying forest cover loss in Democratic Republic of the Congo, 2000-2010, with Landsat ETM+ data. Remote Sens. Environ. 122, 106–116. doi:10.1016/j.rse.2011.08.027

R_Core_team, 2016. R: A Language and Environment for Statistical Computing. R Foundation for Statistical Computing, Vienna, Austria. https://www.r-project.org/.

Ranghetti, L., Busetto, L., 2019. sen2r: Find, Download and Process Sentinel-2 Data. [WWW Document]. R Packag. version 1.1.0. doi:10.5281/zenodo.1240384

Reiche, J., de Bruin, S., Hoekman, D.H., Verbesselt, J., Herold, M., 2015. A Bayesian approach to combine landsat and ALOS PALSAR time series for near real-time deforestation detection. Remote Sens. 7, 4973–4996. doi:10.3390/rs70504973

Reiche, J., Hamunyela, E., Verbesselt, J., Hoekman, D., Herold, M., 2018a. Improving near-real time deforestation monitoring in tropical dry forests by combining dense Sentinel-1 time series with Landsat and ALOS-2 PALSAR-2. Remote Sens. Environ. 204, 147–161. doi:10.1016/j.rse.2017.10.034

Reiche, J., Verhoeven, R., Verbesselt, J., Hamunyela, E., Wielaard, N., Herold, M., 2018b. Characterizing Tropical Forest Cover Loss Using Dense Sentinel-1 Data and Active Fire Alerts. Remote Sens. 2018, Vol. 10, Page 777 10, 777. doi:10.3390/RS10050777

Ryan, C.M., Hill, T., Woollen, E., Ghee, C., Mitchard, E., Cassells, G., Grace, J., Woodhouse, I.H., Williams, M., 2012. Quantifying small-scale deforestation and forest degradation in African woodlands using radar imagery. Glob. Chang. Biol. 18, 243–257. doi:10.1111/j.1365-2486.2011.02551.x

Sentinel-2 PDGS Project Team, 2011. GSC Sentinel-2 PDGS Products Definition Document.

Shimizu, K., Ponce-Hernandez, R., Ahmed, O.S., Ota, T., Chi Win, Z., Mizoue, N., Yoshida, S., 2017. Using Landsat time series imagery to detect forest disturbance in selectively logged tropical forests in Myanmar. Can. J. For. Res. 47, 289–296. doi:10.1139/cjfr-2016-0244

Tang, X., Bullock, E.L., Olofsson, P., Estel, S., Woodcock, C.E., 2019. Near real-time monitoring of tropical forest disturbance: New algorithms and assessment framework. Remote Sens. Environ. 224, 202–218. doi:10.1016/J.RSE.2019.02.003

Verbesselt, J., Hyndman, R., Newnham, G., Culvenor, D., 2010. Detecting trend and seasonal changes in satellite image time series. Remote Sens. Environ. 114, 106–115. doi:10.1016/j.rse.2009.08.014

Verbesselt, J., Zeileis, A., Herold, M., 2012. Near real-time disturbance detection using satellite image time series. Remote Sens. Environ. 123, 98–108. doi:10.1016/J.RSE.2012.02.022

Vicente-Serrano, S.M., Pérez-Cabello, F., Lasanta, T., 2008. Assessment of radiometric correction techniques in analyzing vegetation variability and change using time series of Landsat images. Remote Sens. Environ. 112, 3916–3934. doi:10.1016/j.rse.2008.06.011

White, J.C., Wulder, M.A., Hermosilla, T., Coops, N.C., Hobart, G.W., 2017. A nationwide annual characterization of 25 years of forest disturbance and recovery for Canada using Landsat time series. Remote Sens. Environ. 194, 303–321. doi:10.1016/j.rse.2017.03.035

Wimberly, M.C., Reilly, M.J., 2006. Assessment of fire severity and species diversity in the southern Appalachians using Landsat TM and ETM+ imagery. doi:10.1016/j.rse.2006.03.019

Wulder, M.A., Masek, J.G., Cohen, W.B., Loveland, T.R., Woodcock, C.E., 2012. Opening the archive: How free data has enabled the science and monitoring promise of Landsat. Remote Sens. Environ. 122, 2–10. doi:10.1016/j.rse.2012.01.010

Yan, L., Roy, D.P., Li, Z., Zhang, H.K., Huang, H., 2018. Sentinel-2A multi-temporal misregistration characterization and an orbit-based sub-pixel registration methodology. Remote Sens. Environ.

215, 495–506. doi:10.1016/j.rse.2018.04.021

Zhu, Z., 2017. Change detection using landsat time series: A review of frequencies, preprocessing, algorithms, and applications. ISPRS J. Photogramm. Remote Sens. 130, 370–384. doi:10.1016/j.isprsjprs.2017.06.013

Zhu, Z., Woodcock, C.E., 2014. Automated cloud, cloud shadow, and snow detection in multitemporal Landsat data: An algorithm designed specifically for monitoring land cover change. Remote Sens. Environ. 152, 217–234. doi:10.1016/j.rse.2014.06.012

Zhu, Z., Woodcock, C.E., 2012. Object-based cloud and cloud shadow detection in Landsat imagery. Remote Sens. Environ. 118, 83–94. doi:10.1016/j.rse.2011.10.028

Chapter III - Change detection with BaytsDD and Bayts using the entire time series: overcome the seasonal problem in temperate forest

1 Abstract

Applying forest change detection algorithms developed in tropical forest to temperate forest, such as Italian, it could be a virtuous way to exploit established knowledge on monitoring deforestation to create affordable and reliable inventory tools. European and Italian politicians (European_Commission, 2013), as well as managers and controllers (Mori, 2019) need a practical and reliable way for monitoring forests and harvesting with good temporal and spatial accuracy.

Whole time series change detection approach has the opportunity to reduce tremendously the lag between logging event and remote detection, especially using Sentinel-2 with 5 days revisit time. The main problem with a whole time series in temperate forest is the season effect. This study applied the same change detection method to Italian forest with two different seasonality removal approach. A simpler one with a spatial normalization on 95th percentile and another with harmonic model fitting.

The spatial normalization wasn't able to remove entirely the season effect either on NBR or NDVI time series, causing many commission errors. The Producer Accuracy was very high, but since the model was overestimating the forest disturbed areas, the User accuracy was low. On the other hand, the harmonic model fitting had great potential for seasonality removing, but it required a time period to calibrate the function. This need reduced drastically the monitoring period because the Sentinel-2 time series started on 2015 and ended on 2018.

The harmonic model fitting had encouraging results, and over time, Sentinel-2 time series will become longer, consequently the problem of excluding the starting period for calibration will be reduced. This could enhance the application of time series change detection with almost a near-real time ability in temperate forest, which can improve forest management and decision making with accurate data on harvesting period and areas.

2 Introduction

Over the past 10 years, Earth Observation (EO) has exceeded every expectation and it became a groundbreaking technology for monitoring changes of land surface (Thonfeld et al., 2015). Earth observation allows for repeated, synoptic and consistent measurement of the Earth surface. Moreover, processing a series of EO data is referred to time series analysis (Hostert et al., 2019).

Tropical forest are highly susceptible to anthropogenic degradation and deforestation, hence remote sensing research has been focused to find a reliable and affordable way to assess this type of changes for several decades (Shimizu et al., 2017; Potapov et al., 2012; Asner et al., 2009; Skole and Tucker, 1993).

Traditionally, most of the published literature in remote sensing change detection used bi-temporal method (Zhu, 2017; Thonfeld et al., 2015). But the opening of Landsat data archive in 2008 (Wulder et al., 2012; Woodcock et al., 2008) started to stimulate the use of multitemporal methods rather than bi-temporal, reaching nowadays near-real time performances using time series analysis (Tang et al., 2019; Reiche et al., 2018b; Hirschmugl et al., 2017a; Hamunyela et al., 2016a).

Plenty of literature have already described methods for forest change detection, even using time series, but they have been mainly developed in tropical forest (Reiche et al., 2018a; Hirschmugl et al., 2017b; Ryan et al., 2012; Asner et al., 2009). Tropical forest needs are mainly on a quick identification and quantification of deforestation over large areas, but the importance of sustainable forest management is rapidly increasing in Europe as well. Indeed in the European Commission is raising awareness on this topic (2013), however in Italian forest there is a lack of statistical data on forest harvesting (Mori, 2019), therefore a reliable method for mapping and forest degradation and disturbance identification is essential. On this regard time series analysis could be a reliable and affordable method for monitoring forest harvesting and disturbance with a continuous update.

Beside all the problems already discussed and illustrate in Chapter II2.1 about optical Remote sensing data, the optical images are susceptible of seasonal or cyclic changes driven mostly from annual temperature and rainfall interaction (Verbesselt et al., 2012), which impacts in plant phenology. This is particularly true in temperate zones, where four seasons are remarkably impacting on plant crown appearance and characteristics. For whole time series approach, this seasonal effect was a real concern and had to be addressed.

The Apennine forest is predominantly composed by broadleaf tree, but some planted conifer, such as *Pinus spp, Abies and Picea* are present as well. The forest management in coniferous stands is mainly based on thinning and clear-cut. On the other hand, the principal techniques in broadleaf stands are coppice with standards, conversion from coppice to high forest and thinning. This forest management is very different from the extensive clear-cut or selective logging applied to tropical forest. Often in Italian forest the crown cover is only partially removed during the forest harvesting.

Taking all into account, forest types, seasonal effects as well as degradation drivers, they are all geographic location related, therefore an applicability check on Italian forest of these algorithms is needed. This study aims to compare two methods for forest change detection applied to Italian forest with whole Sentinel-2 time series from 2015 to 2018. These two algorithms overcame the seasonal problem with two different approaches. The first one (Reiche et al., 2018a) was a basic approach using spatial normalization, subtracting the 95^{th} percentile to the pixels values. Instead, the second (Reiche et al., 2018b), it was developed with a data driven approach and it use harmonic model fitting to remove seasonal effect. Both methodologies can lead to a near-real time forest monitoring reducing delays and improving automation in the process compared with single season method (described in Chapter II), hence they are able to fully exploit the Sentinel-2 potential and his short revisit period.

3 Materials and methods

3.1 Study area

The study was conducted in the province of Bologna, which is located in central-north Italy in the Emilia-Romagna region. it's spanning from the Padania flat to the main Apennine rim with an elevation range from few meters to almost 2000m. The area of interest was the same of the previous descripted study, and so it was largely summarized in the Chapter II3.1 and illustrated in Figure 6. It was chosen the same area because of the large dataset already built and checked; having a reliable ground truth dataset with such a spatial and temporal detail was fundamental to calibrate and validate properly the procedures.

3.2 Satellite data

Multispectral optic images collected from Sentinel-2 mission were used to build the time series. The European Space Agency (ESA) started to delivery products from this mission on 04/07/2015, hence this was the starting date of the time series, then the ending date was on 21/09/2018. The whole

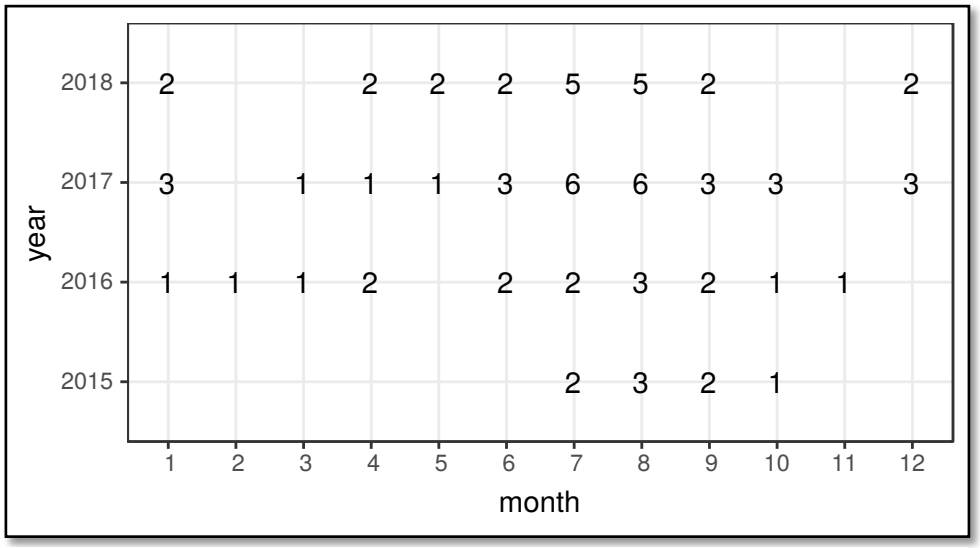

Figure 13 - Number of Sentinel-2 images per month. They represented the whole time series, images with cloud cover lower than 20%. Total amount of image was 76.

time series length was 76 images, it was created with all the images between start and end date beside those with cloud cover above 20%.

The images were downloaded from the Copernicus Open Access Hub thru the API access. Only L1C level products was chosen in order to perform the exact same pre-process workflow to all the images.

Afterward, all pre-process workflow was completed using the "Sen2r" package (Ranghetti and Busetto, 2019) implemented in the R (R_Core_team, 2016) programming language. This package allows to use SEN2COR with some additional options, such as cloud masking and indices calculation. SEN2COR (Main-Knorn et al., 2017; Müller-Wilm, 2017) is an atmospheric correction processor (atmospheric radiative transfer) able to convert L1C products into L2A images. L2A product level is Bottom of Atmosphere (BOA) corrected reflectance image, with terrain and cirrus correction as well. "Sen2r" package was used also for cloud masking, with a 100m buffer and a value of 30 for the buffer smoothing. All the classified scenes (SCL) delivered from SEN2COR processor were applied in the cloud masking (Figure 5). This procedure was adopted despite the possibility of losing "good" pixels because in a time series change detection approach is better a lack of information instead of a wrong pixel value; it could drive to false detection (commission error).

With L2A images time series, Normalized Burned Ratio (NBR)(Key and Benson, 2006) and Normalized Difference Vegetation Index (NDVI) were calculated for their sensitivity to forest disturbance (Shimizu et al., 2017; Grogan et al., 2015). Both indices were calculated despite they are quite similar because after disturbance the NDVI is rapidly rising and tends to saturate easily, while the NBR is more strongly linked to forest structure (White et al., 2017). Moreover they are both widely used in literature for change detection procedures (Lima et al., 2019; White et al., 2017; Cohen et al., 2010; Vicente-Serrano et al., 2008; Wimberly and Reilly, 2006; Cocke A,B et al., 2005).

$$NBR = \frac{NIR - SWIR2}{NIR + SWIR2} \qquad NBR(Sentinel2) = \frac{Band9 - Band12}{Band9 + Band12}$$

$$NDVI = \frac{NIR - RED}{NIR + RED} \qquad NDVI(Sentinel2) = \frac{Band8 - Band4}{Band8 + Band4}$$

Eq. 9 - Normalized Burned Ratio equation with respective band number for Sentinel-2 products (on top), Normalized Difference Vegetation Index equation with respective band number for Sentinel-2 products (o bottom).

3.3 Seasonality removal and pdf estimation for Bayts

In order to apply the change detection procedure developed by Reiche et al. (2018a) on the entire time series the seasonal effect in the indices has to be removed to avoid errors. A spatial normalization was applied following the modified Hamunyela et al. (2016b) procedure described in

the manuscript (Reiche et al., 2018a). The 95th percentile was subtracted to all pixel values, assuming that the upper tail of the distribution (95th percentile) of pixels represents forest pixels (Reiche et al., 2018a; Hamunyela et al., 2016b).

The NF probabilities were computed from probability density functions (pdf), which were derived in different ways for Bayts and BaytsDD. Bayts pdfs were calculated on the calibration dataset built for the study described in the previous Chapter II3.3, hence summarized information on the calibration dataset can be found in Table 6 and Figure 7. Gaussian models were fitted to forest(F) and Non-Forest (NF) distributions from deseasonalized observations.

3.4 Seasonality removal and pdf estimation for BaytsDD

Knowing the harmonic season effect on time series, Reiche et al. (2018b) proposed a more advanced method for removing forest seasonality using an harmonic model fitting. Their technique was applied to the NDVI and NBR time series using a first order harmonic model on the training period. This method doesn't require a calibration dataset, but it needs a training period before the monitoring period. For Sentinel-2 time series this was a real concern since the time series was quite short (from 2015 to 2018), so the training period started from beginning of the time series (2015-07-04) to 2017-07-02 in order to have a good harmonic model fitting. After 2017-07-02 the monitoring phase was started.

For BaytsDD (Data Driven), NBR and NDVI time series were divided in a training period (from beginning to 2017-07-02) and a monitoring period (after 2017-07-02 to end of time series). Beside fitting on the harmonic model for the seasonality removal, the first time series period was used to compute the F median and standard deviation since it was assumed that all observations during the training period represented stable forest. Following the authors guides (Reiche et al., 2018b), Gaussian distributions were applied to describe Forest N(Fmean, 2σ) and Non-Forest N(Fmean-4σ, 2σ) distributions. These values were used from the authors with Sentinel-1 data but looking at the real pixel distribution in the calibration dataset for NDVI and NBR data, their thesis was corroborated and so those values were used to build pdfs for NDVI and NBR as well.

3.5 Bayesian change detection methods: Bayts and BaytsDD

Both change detection methods applied are based on the same probabilistic approach (Reiche et al., 2015a), but they differ on how they remove forest seasonality and how they estimate probability density functions (Reiche et al., 2018a, 2018b). Both methods are pixel-based, and they utilize whole time series for detect forest changes. In this paragraph only a brief description is provided because the probabilistic approach was largely described by Reiche et al. (2015a), the procedure is available as open-source "bayts" package for R (R_Core_team, 2016). The Non-Forest (NF) conditional probability at each time is determinate by iterative Bayesian updating, using previous, current and future observations to confirm or reject a forest disturbance. If the NF condition probability exceeds the defined threshold, a potential disturbance is flagged, in order to be confirmed the follow update has to be over the threshold as well, otherwise the mark will be removed. In this study It was used the default threshold value of 0.9.

3.6 Validation

The validation process followed the most common and applied method in remote sensing change detection (Olofsson et al., 2014; Liu and Zhou, 2004; Macleod and Congalton, 1998). Several error matrices were calculated in order to assess different aspects, such as spatial and temporal accuracy as well as the detection ability for different harvesting techniques. For all the error matrices accuracy parameters were calculated: Producer Accuracy (PA) i.e. the complementary of commission error, User Accuracy (UA) i.e. the complementary of omission error and lastly the Overall Accuracy (OA). The kappa value wasn't intentionally used due to the large number of problems related to this index. A very good explanation on that was given from Olofsson et. al. (2014).

Firstly, the spatial temporal accuracy was verified using a rasterized version of the validation dataset (see Chapter II3.3) applying years as rasterization factor. This raster and the output from the change detection algorithm were compared in the error matrix adopting years (2015 to 2018) as classes plus the not disturbed area (no cut).

Subsequently spatial accuracy excluding the temporal factor was assessed using a simplified validation dataset. All the rasters were simplified in "cut" and "no-cut" classes, as well as the output generated from the change detection algorithm. Then the error matrix was calculated based only on these two simple classes.

Lastly, in order to assess the detection ability for different harvest technique, the validation dataset was modified for each class. For every class (coppice, clear-cut, thinning and conversion) the reference raster and the output raster were masked with the unused classes, e.g. when coppice class was assessed: the clear-cut, thinning and conversion areas were set to no-data in the rasters.

For Bayts procedure the entire validation dataset was used to assess the output, summary information are in Table 11 and the area is illustrated in Figure 7.

Table 11 - Validation dataset summary for Bayts

Type	*Number*	*Average extension (ha)*	*Min extension (ha)*	*Max extension (ha)*	*Total extension (ha)*
Coppice	10	0.62	0.11	1.88	6.2
Clear cut	1	1.15	1.15	1.15	1.15
Thinning	1	2	2	2	2
Conversion	2	3.13	1.26	5.00	6.26
Tot summary	*14*	*1.12*	*0.11*	*5.00*	*15.62*

Instead for BaytsDD the validation dataset wasn't used entirely. Since BaytsDD procedure utilized the first period as training, the monitoring period was started only after 2017-07-02. Consequently, a subset of the validation dataset with only harvesting events executed in the monitoring period was used. Unfortunately, the dataset became quite small with only 3 coppices cut and one clear-cut, considering Sentinel-2 grid (10m spatial resolution), total pixel count per coppice was 98 and 119 pixels for clear-cut.

4 Results and Discussion

Looking at the Figure 14 (B), the seasonality was clearly visible for the NBR time series and NDVI as well. The NBR summer values were about 0.7 but during the winter season they were dropped below 0.1. The Figure 14 illustrate a single pixel trend, but the differences between the two method are visible. Spatial normalization with 95th percentile applied for Bayts method wasn't able to remove entirely the season effect (Figure 14 (A)). On the other hand, fitting a first order harmonic model for BaytsDD was able to remove almost entirely the seasonal effect in the time series (Figure 14 (C)).

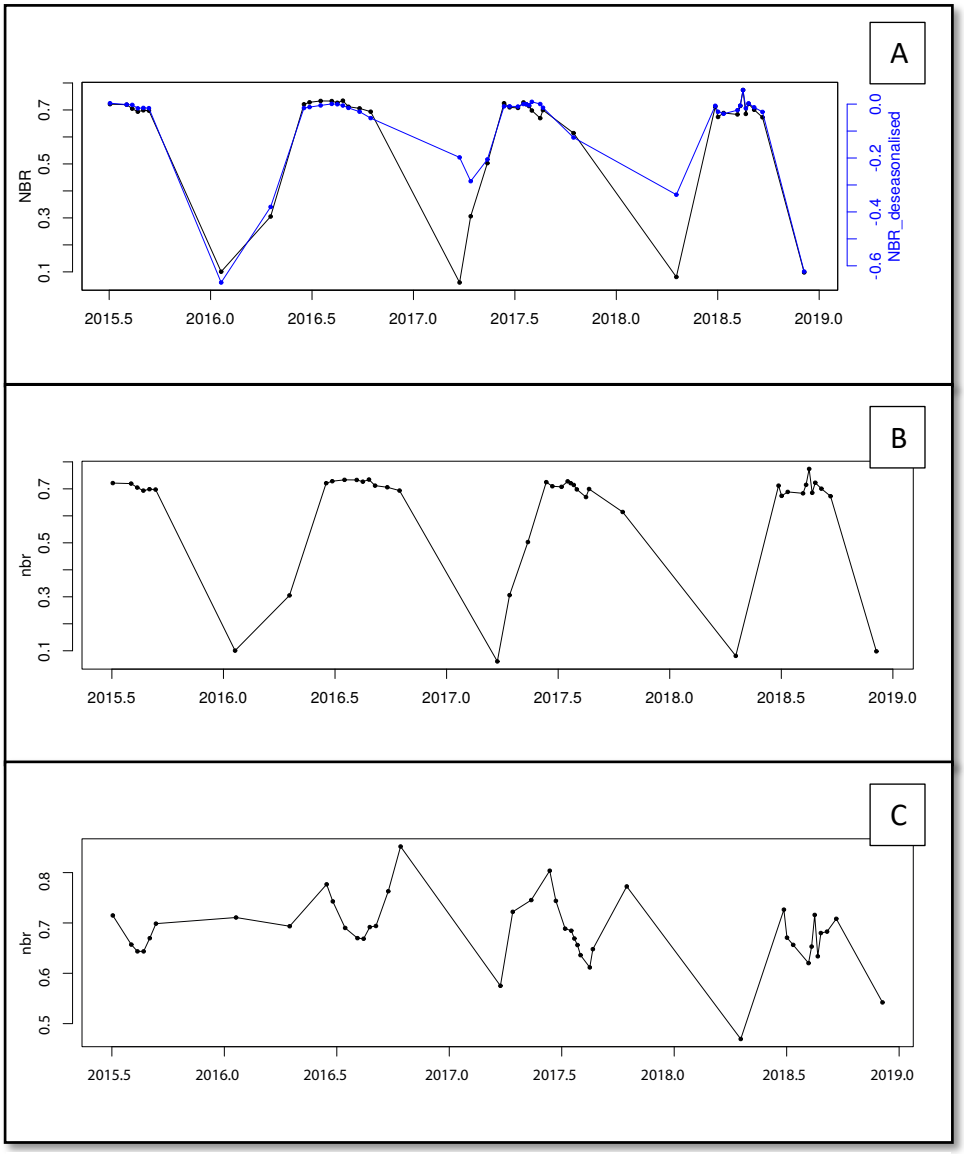

Figure 14 - Deseasonalization for NBR time series in a single pixel with deciduous vegetation. Not deseasonalizated time series in the middle graph (B). The upper graph (A) illustrates both with and without seasonal effect in the NBR time series, the spatial normalization was applied in order to remove the seasonal effect for the Bayts method. The lower graph (C) shows how the harmonic model applied has removed the seasonal effect in the time series, method for BaytsDD.

Moving forward the assessment view from single pixel to raster level, a real comparison between Bayts and BaytsDD results was critical due to the different validation area extension and characteristics. So, discussion for each method was made independently and only carful comments were done for the comparison.

Spatial temporal accuracy assessment revealed very similar results between NDVI and NBR time series in both methods. The Overall Accuracy for Bayts was 78 and 80 using NBR and NDVI respectively, on the other hand, for BaytsDD it was 96 for both NDVI and NBR.

Table 12 - Change detection spatial and temporal assessment for NBR and NDVI time series, both for Bayts and BaytsDD. For BaytDD the monitoring period started in 2017, so the values for 2015 and 2016 were Not Available (NA).

	NBR (Bayts)		*NBR (BaytsDD)*		*NDVI (Bayts)*		*NDVI (BaytsDD)*	
	UA	PA	UA	PA	UA	PA	UA	PA
no cut	99.8	77.7	98.4	98.3	99.8	79.9	98.4	97.9
2015	52.3	98.9	NA	NA	55.0	99.3	NA	NA
2016	39.2	74.8	NA	NA	37.4	71.0	NA	NA
2017	4.0	92.5	73.4	79.5	4.4	91.8	71.0	70.5
2018	2.0	28.6	40.6	37.1	2.2	27.1	29.3	38.6
mean	39.5	74.5	70.8	71.6	39.8	73.8	66.2	69.0

4.1 BaytsDD change detection accuracy

The commission error occurred in BaytsDD deserve a deeper analysis to understand the causes. In the Figure 15 was evident that before the start of monitoring phase, the time series seasonality was very poor due to lack of winter images. This situation leaded to a bad calibration for the harmonic model, which wasn't able to remove the seasonality during the monitoring period and headed to a commission error (low UA value especially in 2018, Table 12).

The low PA value in 2018 was probably due to the distortion inducted from a small validation dataset, in fact, only a single coppice area was present for 2018 and it was identified just partially (Figure 16). This hypothesis was corroborated from data listed in Table 14. PA values for clear cut were very high and for coppice cut were much lower. Beside the distortion inducted from the small reference dataset, this result highlighted the problem of applying change detection algorithm developed for tropical forest to in Italian forest. The clear cut was identified much easier than coppice, which impact less the crown cover.

The simplified assessment method (Table 13) supported the discussion and showed very high OA values (97 for both NBR and NDVI), as well as good results for UA and PA. The model BaytsDD tended to underestimate the total harvesting surface but without high commission error.

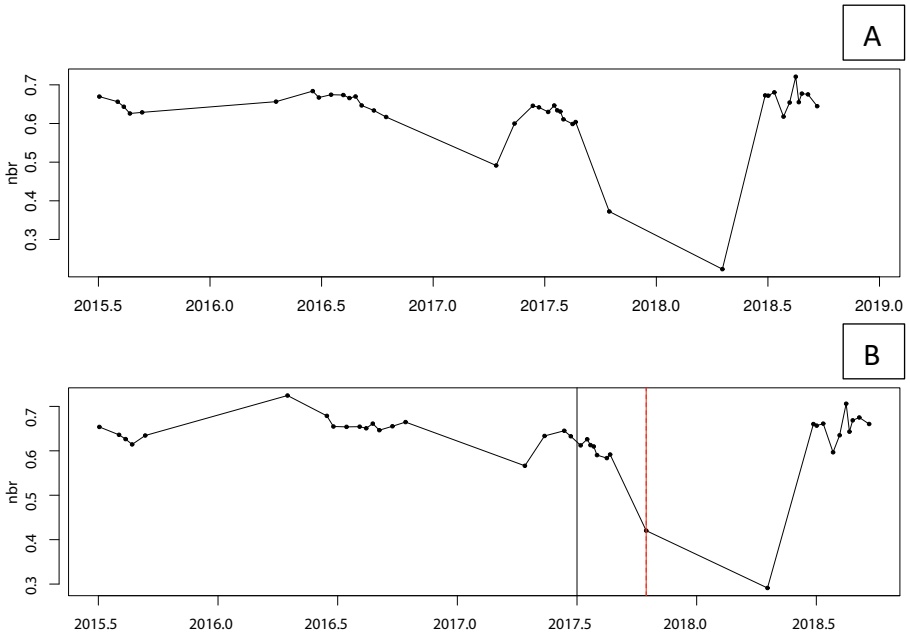

Figure 15 - Single pixel BaytsDD for NBR time series. Detection error occurred due to seasonal removal error. (A) NBR original time series, (B) NBR deseasonalized time series with start monitoring date (black line) and change detection by error (red line).

Table 13 - Simplified assessment for Bayts and BaytsDD using only "cut" and "no-cut" classes.

	NBR (Bayts)		*NBR (BaytsDD)*		*NDVI (Bayts)*		*NDVI (BaytsDD)*	
	UA	PA	UA	PA	UA	PA	UA	PA
no cut	99.8	77.7	98.4	98.3	99.8	79.9	98.4	97.9
cut	21.6	97.9	67.1	69.0	23.2	96.9	63.3	69.4
mean	60.7	87.8	82.8	83.7	61.5	88.4	80.9	83.7

4.2 Bayts change detection accuracy

The seasonal effect showed in Figure 14 and described at the start of this paragraph 4, it had a huge impact in the accuracy assessment. The model was very good at detect the harvested areas (Table 13 high PA cut value) but it wasn't precise in temporal accuracy (Table 12).

Although, the model was overestimating the harvested areas due to false detections. These errors were caused by the incomplete removal of seasonal effect in the time series. Indeed, the seasonal removal failure was evaluated by single pixel time series. Plotting together the original time series and the deseasonalized one (Figure 14 [A]), it was clear that the spatial normalization with the 95th percentile wasn't good enough for remove seasonal effect in temperate forest. The overestimation problem was emphasized in Figure 17 and analytically confirmed by low UA values in all the accuracy tables (Table 12,Table 13,Table 14).

Table 14 - Assessment for verifying the ability to detect changes due to different harvesting techniques. Since the BaytsDD was validated with a smaller validation dataset, only clear cut and coppice were in the dataset and hence for thinning and conversion the results were Not Available (NA).

	NBR (Bayts)			*NBR (BaytsDD)*			*NDVI (Bayts)*			*NDVI (BaytsDD)*		
	UA	PA	OA	UA	PA	OA	UA	PA	OA	UA	PA	OA
Clear cut	51.2	90.3	80.6	81.2	97.1	98.3	51.3	91.2	82.5	79.1	97.0	98.0
Coppice	55.0	88.3	79.7	70.8	67.8	97.5	55.4	88.7	81.6	68.2	68.2	97.2
Thinning	51.6	85.3	80.6	NA	NA	NA	51.8	86.2	82.4	NA	NA	NA
Conversion	55.0	86.9	80.3	NA	NA	NA	55.4	87.4	82.1	NA	NA	NA

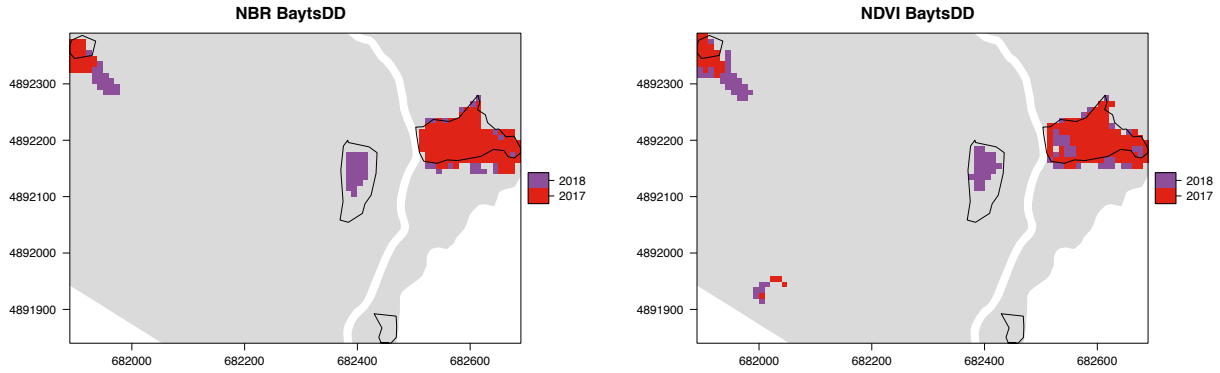

Figure 16 - Output raster from BaytsDD change detection applied to NBR and NDVI time series. Smaller area was used due to the shorter monitoring period.

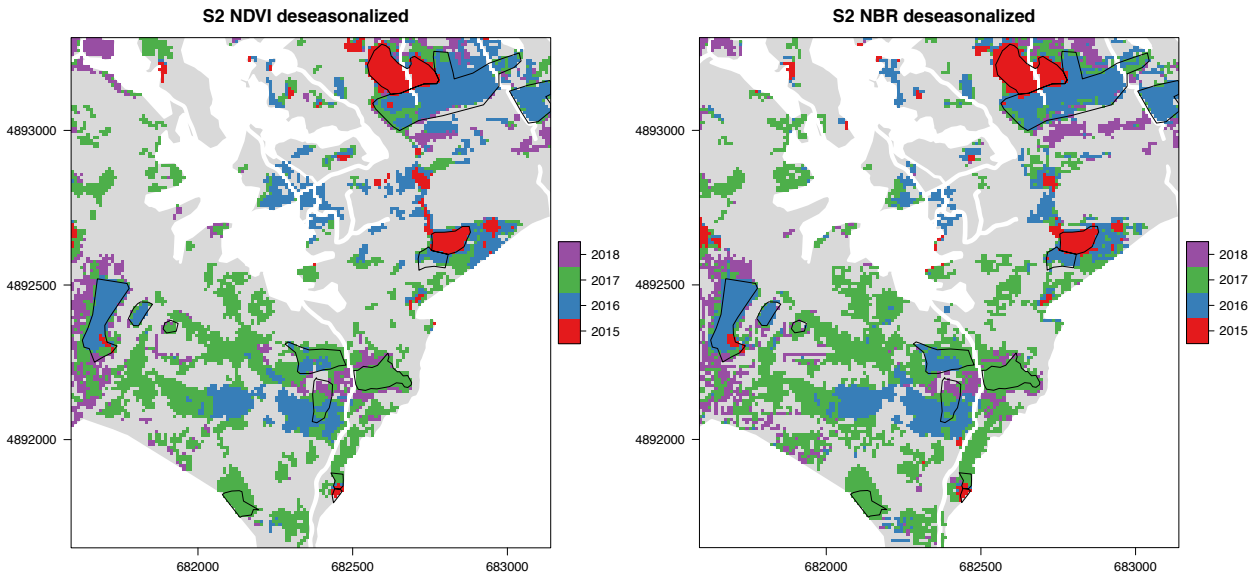

Figure 17 - Output raster from Bayts change detection using NBR and NDVI time series with spatial normalization.

5 Conclusion

The change detection algorithms are applied often on tropical forest (Shimizu et al., 2017; Reiche et al., 2015b; Potapov et al., 2012), and new researches are trying to push forward for fully exploiting new generation remote sensing technologies. Sentinel-2 has very short revisit time (5 days) and open data policy, in this condition the potentials in forest monitoring are very high. Many studies applied different methods to develop near-real time change detection algorithms in tropical forest in order to monitor deforestation (Perbet et al., 2019; Reiche et al., 2018a; Verbesselt et al., 2012). In Italian and temperate forest, the deforestation like in the tropics is not a real concern, nevertheless a carful and sustainable forest management is crucial for maintaining healthy forest and preserve forest for future generation (European_Commission, 2013).

Whole time series change detection approach has the opportunity to reduce tremendously the lag between logging event and remote detection, especially using Sentinel-2 with 5 days revisit time. The results shown in this study confirm the possibility to exploit established knowledge on monitoring deforestation in topical forest to create affordable and reliable inventory tools. The principal obstacle was the seasonal removal process, a precise method had to be applied in order to avoid false detection due to residual seasonal noise. The harmonic model (BaytsDD) revealed very good results and seemed to be able of simulate very well the temperate forest seasonal pattern. But further investigations are needed in order to expand the validation area to corroborate properly this thesis. On the other hand, the spatial normalization (Bayts) on 95^{th} percentile removed the seasonal pattern in time series only partially and this leaded to a very high false detection and commission errors.

Additional investigations and applications are needed before delivering a proper tool for inventories and decision making. The potentials of Sentinel-2 time series and near-real time algorithms are very high for improving the knowledge on temperate forests disturbances and logging activities.

6 Bibliography

Asner, G.P., Knapp, D.E., Balaji, A., Páez-acosta, G., 2009. Automated mapping of tropical deforestation and forest degradation : CLASlite. J. Appl. Remote Sens. 3, 1–24. doi:10.1117/1.3223675

Cocke A,B, A.E., Fulé, P.Z., Crouse, J.E., 2005. Comparison of burn severity assessments using Differenced Normalized Burn Ratio and ground data. Int. J. Wildl. Fire 14, 189–198. doi:10.1071/WF04010

Cohen, W.B., Yang, Z., Kennedy, R., 2010. Detecting trends in forest disturbance and recovery using yearly Landsat time series: 2. TimeSync — Tools for calibration and validation. doi:10.1016/j.rse.2010.07.010

European_Commission, 2013. A new EU Forest Strategy: for forests and the forest-based sector. Brussels.

Grogan, K., Pflugmacher, D., Hostert, P., Kennedy, R., Fensholt, R., 2015. Cross-border forest disturbance and the role of natural rubber in mainland Southeast Asia using annual Landsat time series. Remote Sens. Environ. 169, 438–453. doi:10.1016/j.rse.2015.03.001

Hamunyela, E., Verbesselt, J., Bruin, S. de, Herold, M., 2016a. Monitoring deforestation at sub-annual scales as extreme events in landsat data cubes. Remote Sens. 8. doi:10.3390/rs8080651

Hamunyela, E., Verbesselt, J., Herold, M., Weichelt, H., Griesbach, R., Jonckheere, I., Seifert, F.M., 2016b. Spatio-temporal deforestation monitoring using Sentinel-2, Landsat 7/8.

Hirschmugl, M., Deutscher, J., Gutjahr, K., Sobe, C., Schardt, M., 2017a. Combined Use of SAR and Optical Time Series Data for Near Real-Time Forest Disturbance Mapping, in: 9th International Workshop on the Analysis of Multitemporal Remote Sensing Images. IEEE. doi:10.1109/Multi-Temp.2017.8035208

Hirschmugl, M., Gallaun, H., Dees, M., Datta, P., Deutscher, J., Koutsias, N., Schardt, M., 2017b. Methods for Mapping Forest Disturbance and Degradation from Optical Earth Observation

Data: a Review. Curr. For. Reports 3, 32–45. doi:10.1007/s40725-017-0047-2

Hostert, P., Griffiths, P., Linden, S. van der, Pflugmache, D., 2019. Time Series Analyses in a New Era of Optical Satellite Data, in: Remote Sensing and Digital Image Processing. Springer, pp. 25–41. doi:10.1007/978-3-319-15967-6

Key, C.H., Benson, N.C., 2006. Landscape Assessment (LA).

Lima, T.A., Beuchle, R., Langner, A., Grecchi, R.C., Griess, V.C., Achard, F., 2019. Comparing Sentinel-2 MSI and Landsat 8 OLI Imagery for Monitoring Selective Logging in the Brazilian Amazon. Remote Sens. 11, 961. doi:10.3390/rs11080961

Liu, H., Zhou, Q., 2004. Accuracy analysis of remote sensing change detection by rule-based rationality evaluation with post-classification comparison. Int. J. Remote Sens. 25, 1037–1050. doi:10.1080/0143116031000150004

Macleod, R.D., Congalton, R.G., 1998. A Quantitative Comparison of Change-Detection Algorithms for Monitoring Eelgrass from Remotely Sensed Data. Photogramm. Eng. Remote Sens. 64, 207–216.

Mori, P., 2019. Statistiche forestali: Potenzialità e opportunità per ripartire da zero. Sherwood - For. ed alberi oggi 13–15. doi:ISSN 1590-7805

Olofsson, P., Foody, G.M., Herold, M., Stehman, S. V., Woodcock, C.E., Wulder, M.A., 2014. Good practices for estimating area and assessing accuracy of land change. Remote Sens. Environ. 148, 42–57. doi:10.1016/J.RSE.2014.02.015

Perbet, P., Fortin, M., Ville, A., Béland, M., 2019. Near real-time deforestation detection in Malaysia and Indonesia using change vector analysis with three sensors. Int. J. Remote Sens. 40, 7439–7458. doi:10.1080/01431161.2019.1579390

Potapov, P. V., Turubanova, S.A., Hansen, M.C., Adusei, B., Broich, M., Altstatt, A., Mane, L., Justice, C.O., 2012. Quantifying forest cover loss in Democratic Republic of the Congo, 2000-2010, with Landsat ETM+ data. Remote Sens. Environ. 122, 106–116. doi:10.1016/j.rse.2011.08.027

R_Core_team, 2016. R: A Language and Environment for Statistical Computing. R Foundation for Statistical Computing, Vienna, Austria. https://www.r-project.org/.

Ranghetti, L., Busetto, L., 2019. sen2r: Find, Download and Process Sentinel-2 Data. [WWW Document]. R Packag. version 1.1.0. doi:10.5281/zenodo.1240384

Reiche, J., de Bruin, S., Hoekman, D.H., Verbesselt, J., Herold, M., 2015a. A Bayesian approach to combine landsat and ALOS PALSAR time series for near real-time deforestation detection. Remote Sens. 7, 4973–4996. doi:10.3390/rs70504973

Reiche, J., Hamunyela, E., Verbesselt, J., Hoekman, D., Herold, M., 2018a. Improving near-real time deforestation monitoring in tropical dry forests by combining dense Sentinel-1 time series with Landsat and ALOS-2 PALSAR-2. Remote Sens. Environ. 204, 147–161. doi:10.1016/j.rse.2017.10.034

Reiche, J., Verbesselt, J., Hoekman, D., Herold, M., 2015b. Fusing Landsat and SAR time series to detect deforestation in the tropics. Remote Sens. Environ. 156, 276–293. doi:10.1016/j.rse.2014.10.001

Reiche, J., Verhoeven, R., Verbesselt, J., Hamunyela, E., Wielaard, N., Herold, M., 2018b. Characterizing Tropical Forest Cover Loss Using Dense Sentinel-1 Data and Active Fire Alerts. Remote Sens. 2018, Vol. 10, Page 777 10, 777. doi:10.3390/RS10050777

Ryan, C.M., Hill, T., Woollen, E., Ghee, C., Mitchard, E., Cassells, G., Grace, J., Woodhouse, I.H., Williams, M., 2012. Quantifying small-scale deforestation and forest degradation in African woodlands using radar imagery. Glob. Chang. Biol. 18, 243–257. doi:10.1111/j.1365-2486.2011.02551.x

Shimizu, K., Ponce-Hernandez, R., Ahmed, O.S., Ota, T., Chi Win, Z., Mizoue, N., Yoshida, S., 2017. Using Landsat time series imagery to detect forest disturbance in selectively logged tropical forests in Myanmar. Can. J. For. Res. 47, 289–296. doi:10.1139/cjfr-2016-0244

Skole, D., Tucker, C., 1993. Tropical Deforestation and Habitat Fragmentation in the Amazon: Satellite Data from 1978 to 1988, New Series.

Tang, X., Bullock, E.L., Olofsson, P., Estel, S., Woodcock, C.E., 2019. Near real-time monitoring of tropical forest disturbance: New algorithms and assessment framework. Remote Sens. Environ. 224, 202–218. doi:10.1016/J.RSE.2019.02.003

Thonfeld, F., Hecheltjen, A., Menz, G., 2015. Bi-temporal Change Detection, Change Trajectories and Time Series Analysis for Forest Monitoring. Photogramm. - Fernerkundung - Geoinf. 2, 129–141. doi:10.1127/pfg/2015/0259

Verbesselt, J., Zeileis, A., Herold, M., 2012. Near real-time disturbance detection using satellite image time series. Remote Sens. Environ. 123, 98–108. doi:10.1016/J.RSE.2012.02.022

Vicente-Serrano, S.M., Pérez-Cabello, F., Lasanta, T., 2008. Assessment of radiometric correction techniques in analyzing vegetation variability and change using time series of Landsat images. Remote Sens. Environ. 112, 3916–3934. doi:10.1016/j.rse.2008.06.011

White, J.C., Wulder, M.A., Hermosilla, T., Coops, N.C., Hobart, G.W., 2017. A nationwide annual characterization of 25 years of forest disturbance and recovery for Canada using Landsat time series. Remote Sens. Environ. 194, 303–321. doi:10.1016/j.rse.2017.03.035

Wimberly, M.C., Reilly, M.J., 2006. Assessment of fire severity and species diversity in the southern Appalachians using Landsat TM and ETM+ imagery. doi:10.1016/j.rse.2006.03.019

Woodcock, C.E., Allen, R., Anderson, M., Belward, A., Bindschadler, R., Cohen, W., Gao, F., Goward, S.N., Helder, D., Helmer, E., Nemani, R., Oreopoulos, L., Schott, J., Thenkabail, P.S., Vermote, E.F., Vogelmann, J., Wulder, M.A., Wynne, R., 2008. Free Access to Landsat Imagery. Science (80-.). 320, 1011a-1011a. doi:10.1126/science.320.5879.1011a

Wulder, M.A., Masek, J.G., Cohen, W.B., Loveland, T.R., Woodcock, C.E., 2012. Opening the archive: How free data has enabled the science and monitoring promise of Landsat. Remote Sens. Environ. 122, 2–10. doi:10.1016/j.rse.2012.01.010

Zhu, Z., 2017. Change detection using landsat time series: A review of frequencies, preprocessing, algorithms, and applications. ISPRS J. Photogramm. Remote Sens. 130, 370–384. doi:10.1016/j.isprsjprs.2017.06.013

Chapter IV – Time series change detection with different input sources for assessing increasing spatial resolution: Sentinel-2, CLASlite, RapidEye and PlanetScope

1 Introduction

In remote sensing field there are some technology limitations (Richards and Jia, 2013), but the issue that is most clearly perceived is the spatial resolution. Of course, the satellites equipment are constantly upgraded lunching new carriers and creating new satellite constellations.

The Landsat's satellites, the most famous satellites group, are carrying multispectral optic sensor with 30 m spatial resolution. But nowadays newer satellites with higher spatial resolution are in orbit, such as Sentinel-2, RapidEye and Planet Scope.

The access to these technologies and the calibration/validation dataset at our disposal (Chapter II3.3), they led us to investigate more deeply the effect of spatial resolution in change detection algorithms. In this chapter, the Bayts algorithm (Reiche et al., 2015a) was applied in different time series with the same methodology described in the Chapter II, e.g. using only summer images. The main goals were two, the first was an increasing spatial resolution assessment comparing Sentinel-2 to RapidEye and Planet Scope time series, the second was the implementation of CLASlite software for exploiting the entire electromagnetic spectrum instead of using only normalized indices (Asner et al., 2009).

2 Material and methods

2.1 CLASlite time series

CLASlite is a user-friendly software for automated mapping of tropical deforestation and degradation. This tool was employed in order to build three time series derived from Sentinel-2 (10m pixel) using intermediate CLASlite output. CLASlite is able to calculate for each pixel image the fractional cover for bare soil (S), photosynthetic active vegetation (PV) and non-photosynthetic vegetation as dead or senescent vegetation (NPV). For each Sentinel-2 summer images, already described in the Chapter II3.4, three 38 images long time series were built with S, PV, NPV information. Then, the calibration process was executed independently for each time series

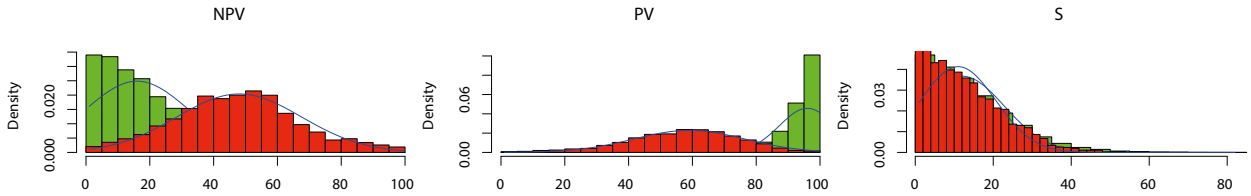

Figure 18 - Calibration probability density function for Forest (green distribution) e Non-Forest (red distribution) area from CLASlite fractional cover. Left: Non-photosynthetic vegetation, Center: Photosynthetic vegetation, Right: Bare soil.

calculating the probability density functions and the needed parameters. All three time series were used together during the Bayts approach (Reiche et al., 2015a), which was able to fuse different time series in a single change detection procedure exploiting information carried from each input.

2.2 Sentinel-2, RapidEye and Planet Scope time series

For Sentinel-2 images the procedure employed for this comparison already descripted in the Chapter II3 in order to create NDVI time series. For the other two satellites, the procedure was replicated but using only images with zero cloud coverage. RapidEye time series was composed of 16 summer images for the NDVI index with a 5m spatial resolution starting in 2014 and ending in 2018. On the other hand, Planet Scope time series started in 2017 and ended in 2018 but a total of 62 images with 3m spatial resolution were downloaded. Unfortunately, since the Planet Scope time series started only in 2017, the Sentinel-2 and RapidEye time series were trimmed to match the same Planet Scope length in order to obtain comparable results. Consequently, in the time period between 2017 and 2018, only 10 images for RapidEye and 27 images for Sentinel-2 were employed for building the time series.

3 Results and Discussion

3.1 CLASlite and Sentinel-2 comparison

The results reached for Sentinel-2 NDVI time series were largely described and discussed in Chapter II4, and the analysis made with CLASlite implementation led to similar problems about false detections for harvest made before the monitoring period. Moreover, the harvest procedure by step in different years was clear in the output map (Figure 19) but decreased significantly the

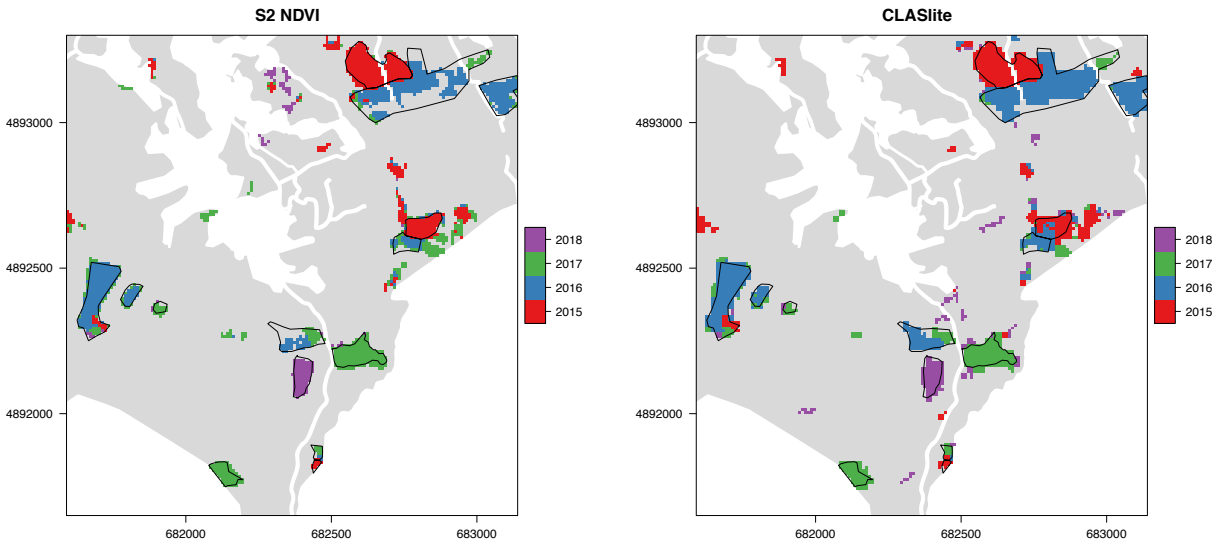

Figure 19 - Bayts change detection comparison between NDVI Sentinel-2 input source (left) and fractional cover from CLASlite (right).

Producer Accuracy especially for the class 2016 in the spatial-temporal assessment (lower in Table 15).

Furthermore, it was noticeable an increment in Producer Accuracy regarding coppice and conversion techniques, although the other harvesting methods were detected in a very similar way with no evident differences between input sources.

In general, outputs from CLASlite fractional cover change detection underlined slight better results, but the improvement is limited for certain classes and often compensated from other. Actually, the Overall accuracy was the same for CLASlite and Sentinel-2 input source: 96.7 spatial assessment and 96 spatial-temporal assessment.

Table 15 - Sentinel-2 NDVI change detection results compared with results obtained using fractional cover time series from CLASlite. Sub-table: Upper for spatial accuracy, center for harvesting technique assessment, lower for spatial-temporal accuracy.

	CLASlite		S-2 NDVI	
	UA	PA	UA	PA
no cut	99.4	97.1	98.8	97.7
cut	65.9	90.2	68.9	80.5
mean	82.7	93.7	83.9	89.1
	UA	PA	UA	PA
Clear cut	60.3	99.1	61.7	99.3
Coppice	73.8	94.8	76.1	93.0
Thinning	63.8	94.1	65.6	94.0
Conversion	75.7	89.1	74.0	79.1
	UA	PA	UA	PA
no cut	99.4	97.1	98.8	97.7
2015	47.8	91.2	57.2	99.6
2016	82.8	73.3	90.1	55.6
2017	32.5	91.8	25.7	91.8
2018	26.6	87.1	49.6	95.7
mean	57.8	88.1	64.3	88.1

3.2 Spatial resolution effect on change detection

The investigation led to similar results with just a few macroscopic differences. The S-2 and Planet Scope time series got a big false detection in 2017 (Figure 20), but actually it was an area harvested the year before (2016). Furthermore, the RapidEye time series wasn't able to detect in an effective way the coppice cut executed in 2018.

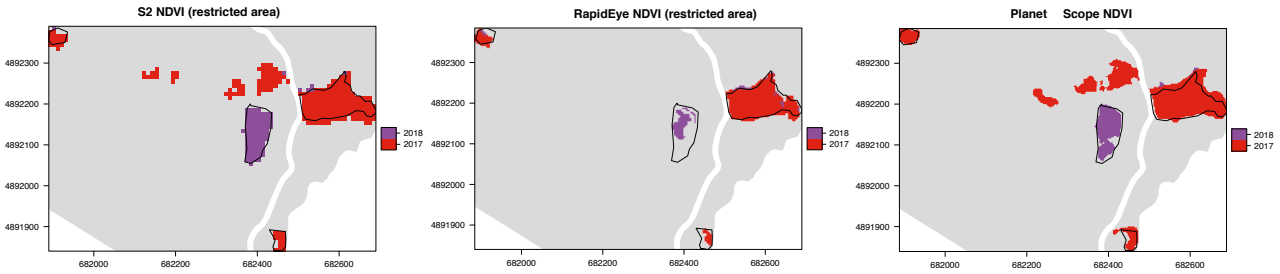

Figure 20 - Bayts change detection mapping with different spatial resolution NDVI time series. input source from Sentinel-2 (10m) on the left, RapidEye (5 m) in center and Planet Scope (3m) on the right.

Since the validation area was quite small and with just four harvested areas, these two little errors effected drastically the accuracy tables. Indeed, the S-2 and Planet Scope false detection have significantly reduced the 2017 class UA values in the spatial-temporal assessment, as well as the coppice omission by RapidEye reduced the PA values in the 2018 class.

However, if we exclude this macroscopic errors, Sentinel-2 time series reached slightly better results than the other time series with higher spatial resolution. This it's probably due to multiple causes such as different revisit time and so different number of images per time series, higher relative error in geolocation accuracy for the images with high spatial resolution it can lead to problems along the borders.

Table 16 - Comparison for spatial resolution increment in change detection algorithm using Sentinel-2 (10m), RapidEye (5m) and Planet Scope (3m) time series. Sub-table: Upper for spatial accuracy, center for harvesting technique assessment, lower for spatial-temporal accuracy.

	S-2 NDVI (10m)		RapidEye NDVI (5m)		Planet Scope NDVI (3m)	
	UA	PA	UA	PA	UA	PA
no cut	99.8	97.1	98.5	99.3	99.6	96.9
cut	63.3	95.8	83.7	71.3	60.2	91.8
mean	81.6	96.5	91.1	85.3	79.9	94.4
	UA	PA	UA	PA	UA	PA
Clear cut	76.7	98.8	90.7	98.2	74.4	97.8
Coppice	75.1	94.4	92.8	70.9	72.9	91.0
	UA	PA	UA	PA	UA	PA
no cut	99.8	97.1	98.5	99.3	99.6	96.9

2017		56.6	94.5	82.6	86.7	52.5	96.3
2018		80.7	95.7	76.8	34.4	92.6	82.5
	mean	79.0	95.8	86.0	73.5	81.6	91.9

4 Conclusion

This little investigation achieved interesting results on the spatial resolution influence to change detection algorithm and the information carried by the CLASlite fractional cover. In the resolution assessment, the validation area limited to such a small extent was useful as a preliminary study and so further investigation with larger areas are needed to confirm these results. However, about the coppice and clear cut seemed that the Sentinel-2 time series with 10m spatial resolution was the better choice and there was no need to improve spatial resolution to gain more accuracy.

On the other hand, the fusion approach with CLASlite reached better results than Sentinel-2 NDVI time series on the ability to detect conversion and coppice harvesting. This was probably due to the information gained from spectral reflectance libraries employed in the CLASlite software.

5 Bibliography

Asner, G.P., Knapp, D.E., Balaji, A., Páez-acosta, G., 2009. Automated mapping of tropical deforestation and forest degradation : CLASlite. J. Appl. Remote Sens. 3, 1–24. doi:10.1117/1.3223675

Reiche, J., de Bruin, S., Hoekman, D.H., Verbesselt, J., Herold, M., 2015. A Bayesian approach to combine landsat and ALOS PALSAR time series for near real-time deforestation detection. Remote Sens. 7, 4973–4996. doi:10.3390/rs70504973

Richards, J.A., Jia, X., 2013. Remote Sensing Digital Image Analysis, Fifth edit. ed, Remote Sensing Digital Image Analysis. Springer Heidelberg, New York, Dordrecht, London. doi:10.1007/978-3-662-03978-6

General conclusion

Earth Observation science had an explosive growth since the policy change on data distribution for Landsat archive (NASA) and the advent of Copernicus program (ESA). Remote sensing science added a new way of looking and studying the earth, a general prospective of the entire globe is necessary for a better understanding of global changes. This quite new technology can be useful in a wide range of forest applications for policy and decision making as well as forest monitoring.

In a global changing framework forests and silviculture play a key role in anthropogenic carbon footprint. With a view of sustainable forest management, forest disturbance monitoring is essential in order to properly understand forest dynamics and exploitation for making the right policy decisions. In a multilevel point of view (global, national and local) having different data spatial resolution is common and usually right, i.e. a global forest change detection with 30m pixel resolution is quite good, instead a national or local tool should have more detailed information.

In this prespective, we applied remote sensing technology to two different aspects about forest decision making (land suitability) and forest harvesting statistics and control. The implementation of Sentinel-2 data allow us to obtain information in a medium-high spatial resolution (10m pixel), which allow studies and evaluation ad national and local scale.

In the first chapter, we have successfully demonstrated the possibility to employ vegetation indices derived from Sentinel-2 for estimating the land suitability for the Douglas fir plantation in Italy. This way wasn't the best in term of accuracy evaluation shown in the study, but it can be an affordable tool for a preliminary assessment. The open access Sentinel-2 policy data encourage hardly this type of application in a local and national scale. With the purpose of green investments and stimulation of wood production for increasing the use of sustainable row materials, Douglas-fir plantations are very high productive in terms of wood volume and quality. Therefore, tools developed and assessed in this study for land suitability and fertility index estimation are ready to be used and they can be very important for leading land management and guide clever investments.

In the second and third chapter, forest change detection from satellite images revealed great opportunity for monitoring forest harvesting and disturbance in Italy. This procedure is well known for monitoring mainly tropical forest on a large scale but applied to Italian forest it can improve drastically the spatial and temporal knowledge on forest harvesting. These information are now crucial for a sustainable forest management and policy decision makers.

If the temporal resolution is not a key point, the method descripted in the second chapter revealed impressive results during the accuracy assessment. This tool is now calibrated and validated on Apennines forest and it can be used locally or applied on a larger scale for gathering information on forest harvesting and help authorities for controlling illegal logging and collecting harvesting statistics.

On the other hand, if temporal accuracy is important and a near- real time forest monitoring is more appropriate, overcame the seasonal noise in the time series is needed. A simple spatial normalization on 95^{th} percentile didn't remove all time series seasonality, but fitting harmonic model shown promising results for temperate forest. Further analyses are needed in order to confirm these results because the validation area was quite small, but encouraging results are shown in the third chapter.

In conclusion, some applicable forest tools were developed and validated for Italian forests with different purposes. This work successfully aimed to integrate and exploit more satellite remote sensing potential to forest management and decision making, simplifying crucial information collection for keeping forest sector into a sustainable path. The application of Sentinel-2 data allowed us to generate very detailed information either spatial and temporal. The Sentinel-2 global covering with such high spatial resolution and short revisit time can be useful for different level application, from local to national and even global scale.